Hänisch, J., Ehinger, J., Ladwein, M., Rohde, M., Derivery, E., Bosse, T., Steffen, A.,
Bumann, D., Misselwitz, B., Hardt, W.D., Gautreau, A., Stradal, T.E., Rottner, K.
Molecular dissection of Salmonella-induced membrane ruffling versus invasion.
(2010) Cellular microbiology, 12 (1), pp. 84-98.

Molecular dissection of *Salmonella*-induced membrane ruffling *versus* invasion

Jan Hänisch[1], Julia Ehinger[2], Markus Ladwein[2], Manfred Rohde[3], Emmanuel Derivery[4], Tanja Bosse[5], Anika Steffen[6], Dirk Bumann[7], Benjamin Misselwitz[8], Wolf-Dietrich Hardt[8], Alexis Gautreau[4], Theresia E.B. Stradal[1], and Klemens Rottner[2,9]

[1]Signalling and Motility Group, [2]Cytoskeleton Dynamics Group, [3]Department of Microbial Pathogenesis, Helmholtz Centre for Infection Research, Inhoffen Strasse 7, D-38124 Braunschweig, Germany; [4]Laboratoire d'Enzymologie et Biochimie Structurales, UPR3082 CNRS - Bat 34, Avenue de la Terrasse, 91198 Gif-sur-Yvette Cedex, France; [5]Institute of Virology, OE 5230, Hannover Medical School, Carl-Neuberg-Strasse 1, D-30625 Hannover, Germany; [6]Faculty of Medicine, Biochemistry I, University of Cologne, Joseph-Stelzmann Strasse 52, D-50931 Cologne, Germany; [7]Infection Biology, Biozentrum, University of Basel, Klingelbergstrasse 50/70, CH-4056 Basel, Switzerland; [8]Institute of Microbiology, ETH Zürich, Wolfgang-Pauli-Strasse 10, CH-8093 Zürich, Switzerland

[9]To whom correspondence should be addressed:

Phone: +49-531-6181-3070

Fax: +49-531-6181-3099

Email: klemens.rottner@helmholtz-hzi.de

Keywords: *Salmonella*, ruffling, WAVE-complex, N-WASP, WASH, Arp2/3-complex

Running title: Separation of *Salmonella*-induced ruffling and entry

Summary

Type III secretion system-mediated injection of a cocktail of bacterial proteins drives actin rearrangements, frequently adopting the shape of prominent protuberances of ruffling membrane, and culminating in host cell invasion of gram-negative pathogens like *Salmonella typhimurium*. Different *Salmonella* effectors are able to bind actin and activate Rho-family GTPases, which have previously been implicated in mediating actin-dependent *Salmonella* entry by interacting with N-WASP or WAVE-complex, well established activators of the actin nucleation machine Arp2/3-complex. Using genetic deletion and RNA interference studies, we show here that neither individual nor collective removal of these Arp2/3-complex activators affected host cell invasion as efficiently as Arp2/3-complex knockdown, although the latter was also not essential. However, interference with WAVE-complex function abrogated *Salmonella*-induced membrane ruffling without significantly affecting entry efficiency, actin or Arp2/3-complex accumulation. In addition, scanning electron microscopy images captured entry events in the absence of prominent membrane ruffles. Finally, localization and RNA interference studies indicated a relevant function in *Salmonella* entry for the novel Arp2/3-complex regulator WASH. These data establish for the first time that *Salmonella* invasion is separable from bacteria-induced membrane ruffling, and uncover an additional Arp2/3-complex activator as well as an Arp2/3-complex-independent actin assembly activity that contribute to *Salmonella* invasion.

Introduction

The actin cytoskeleton of eukaryotes is essential for individual or collective cell motility and for any type of shape change of the cell periphery, induced e.g. by interactions of bacterial or viral pathogens with the plasma membrane of their hosts. As a consequence, numerous regulators of the actin cytoskeleton have previously been implicated as targets of virulence factors of different pathogens, which are abused for the respective pathogen's needs (Munter *et al.*, 2006, Rottner *et al.*, 2005).

Actin filament nucleation in cells is driven by different machines, of which the Arp2/3-complex has until recently received most attention. This complex has emerged as an essential mediator of actin filament generation in processes as diverse as the formation of lamellipodia and ruffles - sheet-like membrane-enclosed protrusions filled with networks of actin filaments, the intracellular movement of bacterial pathogens like *Listeria monocytogenes* or *Shigella flexneri*, or the actin-driven surfing of vaccinia virus and pathogenic *E. coli* on the surface of infected cells (Goley and Welch, 2006). Arp2/3-complex-mediated actin filament assembly involves a conformational change of the complex brought about by so-called nucleation promoting factors (NPFs) harbouring domains essential for Arp2/3-complex and actin binding, the so-called VCA-module (Stradal and Scita, 2006, Takenawa and Suetsugu, 2007). The listerial or rickettsial NPF homologues ActA and RickA, respectively, are capable of Arp2/3-complex activation at the bacterial surface, driving their intracellular motility and cell-to-cell spread independently of any cellular NPF, whereas *Shigella flexneri* or *Mycobacterium marinum* have evolved to exploit the widely expressed N-WASP (neural Wiskott-Aldrich-Syndrome protein) for this purpose (Stevens *et al.*, 2006). Interestingly, actin tail or pedestal formation induced by Vaccinia virus or pathogenic *E. coli* of the EPEC and EHEC type is also exclusively mediated by N-WASP, or its haematopoietic counterpart WASP (Lommel *et al.*, 2004, Lommel *et al.*, 2001, Snapper *et al.*, 2001). In contrast, the

closely related WAVE subfamily proteins that comprise three isoforms in mammals and are essential for Arp2/3-dependent ruffle formation and lamellipodia protrusion have not been implicated in actin tail or pedestal formation (Rottner *et al.*, 2005, Stradal and Scita, 2006).

Another type of actin reorganisation induced and exploited by many bacterial pathogens is the induced phagocytosis of the bacteria into normally non-phagocytic cells, which allows them to invade and spread into cells and tissues, and escape defence forces of the humoral immune system (Cossart and Sansonetti, 2004). *Salmonella typhimurium* certainly constitutes a paradigm of a pathogen following such a strategy, and the invasion process and potential molecular events driving it have therefore been intensely studied. The genus *Salmonella* causes gastroenteritis and typhoid fever in humans and other animals. Invading bacteria deliver effectors directly or indirectly targeting the actin cytoskeleton thought to provoke the protrusion of membrane ruffles and lamellipodia eventually enclosing the bacteria in a process reminiscent of engulfment of large volumes of extracellular medium in macropinocytosis (Schlumberger and Hardt, 2006). The cocktail of bacterial effectors established to effect actin cytoskeleton rearrangements includes three Sops (Salmonella outer proteins) that directly (SopE and E2) or indirectly (SopB) target small GTPases of the Rho family, key upstream regulators of host cell actin rearrangements, as well as SipA and SipC (Patel and Galan, 2005). SopE and SopE2 mimic guanine nucleotide exchange factors (GEFs) capable e.g. of Rac1 and Cdc42 activation (Hardt *et al.*, 1998, Stender *et al.*, 2000), whereas the inositol polyphosphatase SopB activates Rho-GTPases such as RhoG through SGEF (SH3-containing GEF) stimulation by phosphoinositide fluxes (Norris *et al.*, 1998, Patel and Galan, 2006, Zhou *et al.*, 2001). SipC can nucleate and bundle actin filaments directly with domains that are functionally separable from its essential role in effector delivery (Chang *et al.*, 2005, Hayward and Koronakis, 1999). SipA promotes these activities and is also thought to antagonise gelsolin or cofilin-mediated actin filament disassembly (McGhie *et al.*, 2001, McGhie *et al.*, 2004). Cdc42 and Rac GTPases are well established to signal to actin

reorganisation through direct or indirect interactions with the WASP and WAVE families of Arp2/3-complex activators, respectively (Stradal and Scita, 2006). RhoG has been implicated to operate both independently of these GTPases as well as upstream of Rac1 (Katoh and Negishi, 2003, Wennerberg *et al.*, 2002). It is no surprise that the members of these pathways, their collective biochemical functions and those of the delivered bacterial effectors generate a complex network of activities considered to cooperate to promote bacterial entry (Cain *et al.*, 2008, Schlumberger and Hardt, 2006). Both Cdc42/Rac/RhoG GTPases and WASP/WAVE proteins have also previously been implicated in regulating *Salmonella* invasion (Patel and Galan, 2006, Shi *et al.*, 2005, Unsworth *et al.*, 2004). However, it is far from clear how the individual activities of these molecules contribute to both *Salmonella*-induced membrane ruffling and bacterial entry. We have begun to systematically dissect the role of individual constituents of these host signalling pathways by employing RNA interference or cell lines from genetically modified mice. We found that although WAVE operates in *Salmonella*-induced ruffling, WAVE-complex-mediated Arp2/3-complex activation is dispensible for efficient entry. Furthermore, Arp2/3-complex-mediated actin assembly relevant for invasion is driven, at least in part, by the novel Arp2/3-complex activator WASH (Linardopoulou *et al.*, 2007), which appears unable to induce ruffling in the absence of WAVE-complex. Collectively, our data demonstrate for the first time that *Salmonella*-induced ruffling and invasion, both driven by actin polymerisation, can be functionally separated.

Results and Discussion

Salmonella invasion can occur in the absence of WAVE-complex and prominent membrane ruffling.

Considering the importance of exploitation of protein complexes signalling to reorganisation of the actin cytoskeleton in *Salmonella* invasion, we systematically assessed the role of actin regulators established to operate downstream of Rho-family GTPases such as Cdc42 or Rac1, both direct substrates for SopE and SopE2. The ubiquitously expressed members of the WASP/WAVE protein family, N-WASP and WAVE2, effectors for Cdc42 and Rac1, can both be readily recruited to membrane ruffles induced by *Salmonella* (Supplementary Figure 1), similar to previous observations (Unsworth *et al.*, 2004). However, the extent of N-WASP accumulation was more variable than that of WAVE2 (data not shown), which was always recruited to *Salmonella*-induced ruffles (n=30).

Quantification of entry of wildtype *Salmonella typhimurium* into fibroblast cells genetically deficient for the Rho-GTPase Cdc42 (Czuchra *et al.*, 2005) as compared to their parental Cdc42-expressing controls revealed a negligible reduction of invasion (data not shown), as observed previously using RNA interference (Patel and Galan, 2006). Considering this fact, the localization data and the notion that Rac1 knockdown was previously described to cause a reduction in entry (Patel and Galan, 2006), we first focussed on the established Rac effector WAVE-complex. We employed human fibroblast cells (VA-13) stably suppressed for the WAVE-complex constituent Nap1 (Figure 1B), which are also abrogated in expression of other WAVE-complex components (Steffen *et al.*, 2006) and completely deficient in formation of Rac-induced lamellipodia and membrane ruffles (Steffen *et al.*, 2004). These cells were examined for *Salmonella* invasion as compared to mock siRNA-treated cells using a standard gentamicin protection assay (Figure 1A). Surprisingly, stable Nap1 knockdown cells did not display any reduction in invasion rates of wildtype *Salmonella* as compared to

their respective control cells, although the formation of prominent membrane ruffles is considered a key feature of the macropinocytosis-like mechanism of *Salmonella* engulfment. Invasion of *Salmonella* into both cell types was specifically induced by type III secretion system-delivered effector proteins because an isogenic mutant lacking a component of the pore-forming complex of the type III secretion system (ΔSipB) used as non-specific, invasion-deficient control (see Experimental procedures) was abolished in entry (Figure 1A). *Salmonella*-induced ruffling driven by actin polymerisation is thought to mediate bacterial engulfment, so we first examined whether interaction of WAVE-complex-depleted cells (Nap1 RNAi) with *Salmonella* still induced actin accumulation at bacterial entry sites (Figure 2). Interestingly, confocal images of *Salmonella*-infected Nap1 knockdown cells stained for the actin cytoskeleton with phalloidin did reveal actin enrichment at interaction sites between host-cells and bacteria, although prominent ruffles as observed in mock RNAi-treated cells were absent (Figure 2; Supplementary Videos 1 and 2). A similar conclusion could be drawn from images captured by epi-illumination (Supplementary Figure 2). Importantly, no apparent actin accumulations were induced by non-invasive ΔSipB (Supplementary Figure 3). The VA-13 fibroblast cell line stably suppressed for the WAVE-complex subunit Nap1 was previously confirmed to also display downregulated levels of additional complex subunits, including WAVE2 (Steffen *et al.*, 2006). Detailed quantifications revealed Nap1 and WAVE to be expressed at 6.8% and 9.9% of the mock RNAi cell line, respectively, whereas Abi proteins were a bit more abundant (23.5%). To exclude the minute amounts of functional WAVE-complexes in Nap1 knockdown cells to potentially accumulate below *Salmonella* entry sites and drive their uptake, we sought to label these endogenous WAVE-complex subunits with antibodies. Importantly, the WAVE-complex subunit Abi-1 readily co-localized with the ruffles in mock RNAi cells, consistent with the pattern seen for EGFP-tagged WAVE2 (Supplementary Figure 1 and Unsworth *et al.*, 2004), but was completely absent from the

actin accumulations induced by *Salmonella* in Nap1 knockdown cells (Supplementary Figure 4).

However, in spite of the absence of WAVE-complex and prominent ruffles, the polymerisation of actin filaments in these conditions presumably involved the Arp2/3-complex, since antibodies specific for this actin nucleating machine as exemplified here for the smallest Arp2/3-complex subunit ArpC5 (also known as p16) prominently labelled *Salmonella* entry sites (Figure 3). As for actin, Arp2/3-complex accumulation both with or without WAVE-complex specifically required bacterial effector delivery, since no recruitment was observed for ΔSipB bacteria (Supplementary Figure 5).

Together, these data suggest that as opposed to previous proposals (Shi *et al.*, 2005), neither WAVE nor any other member of the WAVE-complex has an essential role in *Salmonella typhimurium* entry and actin or Arp2/3-complex accumulations accompanying entry, at least in the fibroblast cell lines employed here. However, we do acknowledge that a potential relevance of WAVE-complex - and thus ruffling - could also vary with cell type and/or conditions. First, transient as opposed to stable Nap1 knockdown (see above) appeared to very modestly reduce entry efficiency (see e.g. Supplementary Figure 7). Furthermore, strongest effects of Abi-1/WAVE-complex knockdown in previous studies were observed in Hela cells (Shi *et al.*, 2005), and indeed, Nap1 knockdown seemed to affect entry in this cell type more evidently than in fibroblasts, although it certainly did not abolish it (our own unpublished data).

Host cell penetration with and without ruffling.

To obtain a more mechanistic view of the entry process, both in the presence and absence of functional WAVE-complex, Nap1 RNAi and control cells were infected with *Salmonella* and subjected to scanning electron microscopy (Figure 4). Mock siRNA-treated cells displayed gross morphological changes of the cell periphery, with large membrane ruffles seemingly

folding around the bacteria during entry, as one would expect (Patel and Galan, 2005, Rottner *et al.*, 2005, Schlumberger and Hardt, 2006). Entry events captured in Nap1 knockdown cells appeared fundamentally different. There was a clear lack of prominent ruffles (for representative image see Figure 4). Instead, bacteria appeared to fall or dive into the host cell by a "zipper"-like mechanism, reminiscent of what is known from *Listeria* and *Yersinia* species (Cossart and Sansonetti, 2004). Interestingly, similar entry events occurring in the absence of prominent membrane ruffling could also occasionally be captured in control cells (data not shown), as noted previously (Stender *et al.*, 2000), indicating perhaps that the mechanism observed upon WAVE-complex suppression reflects a common mode of bacterial entry mostly masked in the control situation by excess WAVE-complex-dependent membrane ruffling.

Of note, two recent studies also add to evidence in favour of at least partial uncoupling of ruffling and entry efficiencies, though employing distinct experimental settings. First, SipA deletion in the context of different *Salmonella* strains had quite prominent impact on entry efficiency, but not ruffling frequency. Only in strains naturally lacking SopE, such as F98, or in isogenic SL1344 mutants lacking both SopE and SipA the authors concluded ruffle shapes to be changed and to contain increased filopodia numbers (Perrett and Jepson, 2009). Furthermore, a ubiquitination-deficient SopB variant that remains trapped in the plasma membrane induced exaggerated membrane ruffling, but did not outperform wildtype SopB in mediating entry (Patel *et al.*, 2009). Thus, the induction of ruffling does not necessarily promote entry or increase entry efficiency, and conversely, our studies suggest that ruffling can be dispensable for uptake.

Together, these data question the view that *Salmonella*-induced ruffling and entry are driven by identical host cell machineries, and call for a revision of conclusions on the entry machinery exclusively derived from examination and quantification of ruffling.

N-WASP is dispensable for Salmonella entry and does not compensate for WAVE-complex loss of function.

The Cdc42-interacting protein N-WASP has previously been implicated in *Salmonella* invasion, based largely on the expression of dominant negative mutants of the protein (Unsworth *et al.*, 2004), and on the assumption of the engagement of an activator of Arp2/3-complex downstream of this GTPase (Schlumberger and Hardt, 2006). However, this argument is weakened by the observation of a minor role of Cdc42 in the entry of wildtype *Salmonella* (our unpublished data and Patel and Galan, 2006). Thus, the function of N-WASP in *Salmonella* invasion was re-evaluated by the use of cells genetically depleted for the ubiquitously expressed N-WASP (Lommel *et al.*, 2001), which also lack expression of any functional levels of its haematopoietic relative WASP (Benesch *et al.*, 2002). To our surprise, N-WASP knockout cells exhibited a statistically significant increase in entry, indicating that its presence counteracted rather than promoted actin polymerisation driving entry of wildtype *Salmonella* (Figure 5).

These observations demonstrated that individual interference with neither WAVE-complex nor N-WASP abolished *Salmonella* entry. However, these data did not exclude potential functional redundancies of these Arp2/3-complex activators in bacterial invasion. To explore this possibility, we performed transient knockdown of the WAVE-complex component Nap1 in N-WASP-deficient cells. Interestingly, *Salmonella* entry was not significantly reduced after simultaneous removal of both class I Arp2/3-complex activators (Figure 6). As expected, Nap1 knockdown reduced expression of Nap1 and the ubiquitously expressed WAVE2 isoform, but not of Arp2/3-complex (Figure 6). This is in line with the observation of Arp2/3-complex recruitment to sites of *Salmonella* engulfment, again effector delivery-dependent (Supplementary Figure 6), in both mock and Nap1 RNAi-treated N-WASP-deficient cells (Figure 7), suggesting that (an) additional Arp2/3-complex activator(s) must operate in Arp2/3-complex activation at sites of *Salmonella* attachment and internalisation (see also

below). We can already exclude cortactin to have a significant function in this process, since interference with cortactin function was also observed to increase rather than decrease bacterial entry (Unsworth *et al.*, 2004 and our own unpublished data). The observed modest reduction of *Salmonella* invasion upon transient WAVE-complex knockdown in N-WASP knockout cells was independent of the presence of N-WASP, since a similar subtle reduction was observed upon Nap1 RNAi in the parental control fibroblasts expressing N-WASP (Supplementary Figure 7).

However, since N-WASP knockout cells deprived for WAVE-complex expression (Figure 6) engulfed *Salmonella* with higher efficiency than N-WASP- and WAVE-expressing control cells (Figure 5), we conclude that none of these Arp2/3-complex activators can indeed exhibit a quantitatively relevant role in Arp2/3-complex activation accompanying the invasion of wildtype *Salmonella*. This is supported by the observation of Arp2/3-complex accumulation at sites of *Salmonella* entry in both N-WASP knockout cells and the same cells additionally suppressed for WAVE-complex (Figure 7).

Together, our data reveal that neither one of the classical Arp2/3-complex activators N-WASP and WAVE is essential for host cell entry of the wildtype variant of this pathogen. Comparison of our observations with previously published data uncovers potential technical caveats with employing over-expression of dominant negative variants of Arp2/3-complex activators, which is prone to indirect interference with pathways additional to the given dominant negative factor, potentially complicating interpretation. This might be at the foundation of the continuous discrepancies reported for observations obtained with dominant negative approaches *versus* genetic deletions (see e.g. Czuchra *et al.*, 2005, Heasman and Ridley, 2008, Wang and Zheng, 2007, Wheeler *et al.*, 2006).

Arp2/3-complex is involved in but not essential for Salmonella invasion.

Salmonella internalisation was consistently accompanied by Arp2/3-complex enrichment at bacterial entry sites, both in the control situation, and upon individual or collective removal of the Arp2/3-complex activators N-WASP and WAVE-complex (Figures 3 and 7). Previous studies concerning the role of the complex in the invasion of wildtype *Salmonella* employed Arp2/3-complex sequestration in the host cell cytosol by ectopic expression of the C-terminal, Arp2/3-binding domain of Scar1/WAVE1 (Criss and Casanova, 2003, Unsworth *et al.*, 2004). The same approach was successfully used for instance to block lamellipodia formation and membrane ruffling (Machesky and Insall, 1998), actin-based *Listeria* movement (May *et al.*, 1999), or actin polymerisation accompanying clathrin-mediated endocytosis (Benesch *et al.*, 2005). However, Arp2/3-complex sequestration may lead to interference with the function of additional regulators of *Salmonella* invasion, for instance Arp2/3-complex interactors that could contribute to the Arp2/3-complex sequestration phenotype. To exclude this possibility and to unearth additional, independent evidence for a *bona fide* involvement of Arp2/3-complex in the invasion of *Salmonella*, we suppressed two independent subunits of Arp2/3-complex by RNA interference. Owing to reasonable knockdown efficiency and the availability of antibodies to document knockdown efficiency, we chose to suppress both Arp3 and again the more peripheral Arp2/3-complex subunit p21. Importantly, both treatments have previously been observed to abrogate lamellipodia formation and membrane ruffling (Steffen *et al.*, 2006), and are therefore considered a specific and effective method to block Arp2/3-complex function. As observed before (Di Nardo *et al.*, 2005, Steffen *et al.*, 2006), Arp3 knockdown also suppressed p21 expression, but not *vice versa* (Figure 8). Interestingly, transient Arp2/3-complex knockdown consistently reduced the efficiency of *Salmonella* invasion by approximately 50% (Figure 8) in N-WASP-expressing control fibroblasts (N-WASP$^{flox/flox}$). These data suggest a specific and significant contribution of the actin nucleation activity of Arp2/3-complex to *Salmonella* invasion, consistent with its prominent

accumulation at bacteria entry sites (Figures 3 and 7). However, comparison with functional interference studies with the ubiquitous members of the WAVE and WASP families (Stradal and Scita, 2006) reveals that an additional Arp2/3-complex activator must be at play to explain for both the prominent role of Arp2/3-complex in untreated cells and the enrichment of the complex in the absence of WASP and WAVE subfamily proteins (see below).

Interestingly, effects of Arp2/3-complex knockdown were comparable in the presence and absence of N-WASP (Figure 8A). The modestly less penetrant phenotype in N-WASP$^{del/del}$ cells (reduction of bacterial entry by app. 40%) is likely due to slightly lower knockdown efficiency (Figure 8B).

In addition, the efficiency of interference with entry in both cell types, which is quantitatively comparable to Arp2/3-complex sequestration (Criss and Casanova, 2003, Unsworth *et al.*, 2004), indicates an additional, Arp2/3-complex-independent pathway of actin nucleation operating in *Salmonella* invasion, which awaits further characterisation. This pathway requires active actin polymerisation, since treatment with latrunculin B (LatB) that sequesters actin in a non-polymerisable form was confirmed to abolish *Salmonella* entry completely (Supplementary Figure 8), as expected.

Identification of a novel Arp2/3-complex activator operating in Salmonella invasion.

N-WASP and WAVE belong to a group of Arp2/3-complex activators that share a common carboxy-terminal VCA-domain (**V**erprolin homology/WH2, **C**onnector, **A**cidic) (Stradal and Scita, 2006). Owing to the recognition of Arp2/3-complex activation by WHAMM (WASP homolog associated with actin, membranes, and microtubules) (Campellone *et al.*, 2008), the p53-cofactor JMY (Zuchero *et al.*, 2009), and WASH (**W**iskott-**A**ldrich Syndrome Protein and **S**CAR **H**omolog) (Linardopoulou *et al.*, 2007), this protein family has now significantly grown.

To explore a potential involvement of these novel factors in *Salmonella* invasion, we sought initially to study the potential recruitment of these factors to sites of *Salmonella* attachment or invasion. Similar to N-WASP and WAVE2 (Supplementary Figure 1), fibroblasts expressing EGFP-tagged variants of these proteins were subjected to *Salmonella* infection assays, and counterstained for the actin cytoskeleton and bacteria. EGFP-WHAMM prominently targeted to vesicular structures, as expected (Campellone *et al.*, 2008), but not to *Salmonella*-induced ruffles (Figure 9). Likewise, JMY did also not convincingly accumulate at bacterial entry sites. In contrast, cells expressing EGFP-WASH showed clear examples of close association with bacterial entry sites (Figure 9), but interestingly, this accumulation was less stringently associated with ruffling structures as observed for WAVE2 (Supplementary Figure 1). These data indicated a potential involvement of WASH in *Salmonella*-induced Arp2/3-complex activation, independent of induction of prominent membrane ruffling. To directly test for an involvement of WASH in *Salmonella* entry, WASH expression was knocked down by RNA interference in fibroblasts. To our surprise, screening of data from array expression analyses revealed a significant increase of WASH mRNA in three independently generated N-WASP-deficient cell lines as compared to their parental N-WASP-expressing controls (data not shown). Moreover, semi-quantitative Western Blotting confirmed WASH protein to be roughly doubled in amount in the N-WASP-deficient cell line employed here (Figure 10A). To this end, the efficiency of *Salmonella* invasion upon WASH knockdown was tested in both control and N-WASP-deficient cells. Interestingly, invasion was reduced in both cell lines in a statistically significant fashion, although the phenotype was more penetrant in the absence of N-WASP (Figure 10B). Together, these data strongly suggest WASH to constitute a novel Arp2/3-complex activator operating in *Salmonella* invasion.

Concluding remarks.

Our results have important implications for our molecular and mechanistic understanding of the cellular processes driving actin-dependent internalisation of *Salmonella*. Although the entry process triggered by this pathogen is generally considered as the paradigmatic example of a bacterium inducing actin remodelling events into large leaflets of plasma membrane, commonly found for instance during macropinocytosis, our observations reveal for the first time that the formation of these ruffles is not essential for entry. Thus, our experiments add to increasing evidence that suggests separability of *Salmonella* - induced membrane ruffling and host-cell invasion, the former but not the latter essentially requiring the Arp2/3-complex activator WAVE. Furthermore, we confirm a contribution for the Arp2/3-complex in *Salmonella* invasion, but our data also highlight an actin-dependent, Arp2/3-complex-independent aspect of invasion that deserves further investigation. Last, but not least, we define a role in entry for a novel Arp2/3-complex activator, WASH, which appears to accumulate at *Salmonella* entry sites, and may contribute – at least in part – to Arp2/3-complex-dependent actin assembly driving invasion independent of ruffling. If the observed stimulation of *Salmonella* entry by N-WASP removal is causally linked to increased WASH expression remains just one aspect of future investigation.

Experimental Procedures

Bacterial strains

Salmonella enterica serovar Typhimurium SL1344 (Hoiseth and Stocker, 1981), and its isogenic derivative lacking SipB (ΔSipB) were grown in Luria–Bertani (LB) medium according to standard protocols. The ΔSipB strain was constructed using red recombinase-mediated homologous recombination of a linear PCR fragment (Datsenko and Wanner, 2000) carrying a kanamycin-resistance cassette and terminal 40 bp regions homologous to flanking sequences of the sipB gene generated using primers available at http://falkow.stanford.edu/whatwedo/wanner/stmA.primers. The kanamycin cassette was subsequently removed using flp recombinase as described (Datsenko and Wanner, 2000) to minimize polar effects on downstream genes. Indeed, proteome analysis of culture supernatants revealed a lack of SipB but unaltered expression and secretion of SipC, SipD, and SipA (as well as InvJ, SptB, SopB, SopE, and SopE2) (data not shown).

Plasmids, cells, transfections and RNA interference

EGFP-tagged N-WASP and -WAVE2 were as described (Benesch *et al.*, 2002, Lommel *et al.*, 2001). EGFP-WHAMM was kindly provided by Ken Campellone and Matt Welch (University of California, Berkeley) (Campellone *et al.*, 2008). Full length, murine p53-cofactor JMY was amplified from EST clone IRAKp961B15195Q (Resource Centre of the German Human Genome Project, RZPD, Berlin) using primers 5'-GAGAAGATCTATGTCGTTCGCGCTGGAGGAG-3' and 5'-GAGTGAATTCCTAGTTCTCCCAGTCTGTGCAC-3', and fused into vector pEGFP-C1 (Clontech, Mountain View, CA, USA).

Control (N-WASP$^{flox/flox}$) and N-WASP knockout (N-WASP$^{del/del}$) fibroblast cell lines were grown as described (Lommel *et al.*, 2001). Murine NIH 3T3 fibrobasts (ATTC CRL-1658) were grown in DMEM (Invitrogen, Germany) containing 10% FBS (Sigma-Aldrich, Germany), glutamine (2mM), non-essential amino acids (0.1mM) and sodium-pyruvate (1mM) (all Invitrogen, Germany). NIH 3T3 cells were transiently transfected using FuGene6 (Roche Diagnostics, Mannheim, Germany) according to manufacturer's protocols. 3T3 cells stably expressing EGFP-tagged WASH will be described elsewhere (Derivery et al., in revision). VA-13 human lung fibroblasts (ATCC CCL-75.1) mock-treated or stably suppressed for Nap1 expression were described (Steffen et al., 2006). Transient RNAi-mediated knockdown of Nap1 or the Arp2/3-complex subunits Arp3 and Arp-C3 (p21) in control or N-WASP knockout fibroblasts was done with pSUPER.retro.puro derivatives mediating respective shRNA expression as described (Steffen *et al.*, 2006, Steffen *et al.*, 2004). Knockdown vectors were transfected using FuGENE 6 (Roche, Germany) according to manufacturer's protocols, and cells used for invasion assays or immunolabelling experiments at day 4 after transfection.

For WASH knockdown, cells were transfected with 40nM of non-targeting control or ON-TARGET*plus* siRNA (sense: GAAUACGGCUCCAUCUUUAUU, antisense: 5'-P UAAAGAUGGAGCCGUAUUCUU; Dharmacon Inc., Chicago, USA) using Lipofectamine RNAiMAX (Invitrogen, Germany, reverse transfection protocol), re-transfected the next day using forward transfection, and a third time again a day later with reverse transfection. Cells were seeded into 24-well plates two days later and subjected to infection experiments within 24 hours, thus within 5 days after the first siRNA transfection.

Gentamicin protection assays

Bacterial invasion was quantified using the gentamicin survival assay essentially as described previously (Elsinghorst, 1994). In brief, VA-13, siRNA-treated or untreated N-WASP control and knockout cell lines were seeded into 24-well plate-holes at a concentration of app. 1 x 10^5 cells / well, resulting in a confluent cell layer ready for infections within 24 hours. For Nap1 RNAi, N-WASP$^{flox/flox}$ or N-WASP$^{del/del}$ cells were seeded 24 hours after transfection with the respective knockdown vector into selection medium containing 5µg/ml puromycin. Here, cells were seeded into 24-well plate holes at a concentration resulting in a confluent cell layer approximately 72 hours after start of selection. For inhibition of actin polymerisation in Supplementary Figure 8, cells were treated with latrunculin B (LatB; Biomol Research Laboratory, Hamburg, Germany) at 10µM or vehicle as control for 60 minutes prior to infection. LatB treatments were confirmed to effectively depolymerise actin filaments in this cell type by fixation and phalloidin stainings of parallel samples (data not shown).

For infections, bacteria were grown for 16 hours in LB medium, diluted 1:33 into the same medium and cultured for another 3 hours, harvested by centrifugation at 3000 x g for 3 minutes, washed with phosphate buffered saline (PBS), and diluted 1:100 into growth medium (for eukaryotic cells). 1 ml of the diluted bacterial suspension was used for each 24-well plate hole. Infection was initiated by centrifugation (4 minutes at 650 x g) of the bacteria onto eukaryotic cells. After 20 minutes of infection (37°C, 7.5% CO2), cells were washed twice with PBS or CO_2-equilibrated growth medium, and incubated for another 90 minutes in growth medium containing 50µg/ml gentamicin. Subsequently, cells were washed three times with PBS and lysed at 4°C using 0.2% Triton X-100. Diluted lysates were plated onto LB-agar plates for quantification, and invasion efficiency determined and expressed as colony forming units normalised to respective control samples. Equal amounts of eukaryotic cell extracts were determined and ensured by Western blotting of infected samples treated in parallel. Experiments were repeated at least four independent times, and normalised to an

invasion of 1 (100%) in respective control populations as indicated. Data were processed using Microsoft Excel 9.0 (Redmond, WA, USA). Invasion rates were statistically compared as indicated using two-sample two-sided t-tests. Statistical analyses were carried out using Minitab 10.5 (Minitab, State College, PA, USA).

Antibodies, Western Blotting and Immunofluorescence

Polyclonal anti-WAVE2 antibodies were raised against synthetic peptide NH2-EKKDNPNRGNVNPRKIKTRKEEWEKM-COOH and affinity purified using the same peptide immobilized on CNBr-Sepharose 4B (Amersham Biosciences, Little Chalfont, Buckinghamshire, UK). Polyclonal anti-N-WASP (Lommel *et al.*, 2004), anti-Nap1 (Steffen *et al.*, 2004), anti-Arp3 (Steffen *et al.*, 2006) and anti-ArpC3 (p21) (Pistor *et al.*, 2000) antibodies were as described. Monoclonal anti-Abi-1 antibody (clone W8.3) was kindly provided by Giorgio Scita, Milan, Italy (Innocenti *et al.*, 2004). Polyclonal anti-WASH antibodies will be described elsewhere (Derivery et al., in revision). Monoclonal anti-tubulin antibody (clone 3A2) was purchased from Synaptic Systems (Göttingen, Germany). Immunoblotting was performed using enhanced chemiluminescence according to standard protocols. For quantification of WASH protein, band intensities were measured and normalized to tubulin control using AIDA software (Raytest, Straubenhardt, Germany), and averaged from two independent experiments.

For immunofluorescence microscopy, cells were plated onto acid-washed glass coverslips coated with 50µg/ml fibronectin (Roche Diagnostics, Mannheim, Germany) and overlaid with *S. typhimurium* wildtype or the isogenic ΔSipB mutant essentially as for gentamicin protection assays. After 10 minutes of infection, cells were fixed with formaldehyde (PFA, 4%) in phosphate-buffered saline (PBS) for 20 minutes, and extracted with 0.1% Triton X-100 in 4% PFA for 1 minute. For visualisation of the actin cytoskeleton and Arp2/3-complex recruitment during *Salmonella* entry, fixed samples were washed and triple-stained with

phalloidin, monoclonal anti-ArpC5 (p16) antibodies and polyclonal anti-*Salmonella* antibodies. Alexa dye-labelled secondary antibodies and phalloidin were purchased from Invitrogen (Karlsruhe, Germany), and used in colour combinations Alexa Fluor 350, -488 and -594. Polyclonal rabbit anti-*Salmonella* O-antigen group B serum was from Difco Microbiology (Voigt Global Distribution Inc., Kansas, USA), monoclonal anti-ArpC5 (p16) antibodies (clone 323H3) were as described (Olazabal *et al.*, 2002), and purchased from Synaptic Systems (Göttingen, Germany). Epifluorescence imaging was done on an inverted microscope (Axiovert 100TV; Carl Zeiss, Jena, Germany) equipped with a 100x/1.3NA PlanNeofluar objective and for wide-field illumination essentially as described (Steffen *et al.*, 2004). Samples were acquired with a back-illuminated charge-coupled device camera (TE-CCD 800PB; Princeton Scientific Instruments, Princeton, NJ, USA) driven by IPLab software (Scanalytics Inc., Fairfax, VA, USA). For confocal microscopy, samples were processed as above, except that dye-colour combinations were Alexa Fluor 488 and -568 combined with Cy^{TM}5-labelled antibodies (Jackson ImmunoResearch Laboratories Inc., Suffolk, UK), which were excited with laser lines 488, 561 and 632, respectively. Confocal microscopy was performed on a Fluoview1000 using a 100x/1.3NA Plan-Neofluar or a 100x/1.45NA PlanApo TIRF objective (Olympus Inc., Hamburg, Germany). Image acquisition and 3D reconstructions were done using FV10-ASW 1.07 software (Olympus). All microscopy images were processed further with Adobe Photoshop 7.0/CS software (Adobe Systems, Mountain View, CA, USA).

Field emission scanning electron microscopy (FESEM)

Samples were fixed with 2% glutaraldehyde and 5% formaldehyde in cacodylate buffer (0.1M cacodylate, 0.01 M $CaCl_2$, 0.01 M $MgCl_2$, 0.09 M sucrose, pH 6.9) for 1 hour on ice, washed with TE-buffer (20 mM TRIS, 1 mM EDTA, pH 6.9) before dehydrating in a graded series of acetone (10, 30, 50, 70, 90, 100%) on ice for 15 minutes for each step. Samples were then critical-point dried with liquid CO_2 (CPD 30, Bal-Tec, Liechtenstein) and covered with a gold film by sputter coating (SCD 500, Bal-Tec, Liechtenstein) before examination in a field emission scanning electron microscope (Zeiss DSM 982 Gemini) using the Everhart-Thornley SE-detector and the inlens SE-detector in a 50:50 ratio at an acceleration voltage of 5 kV at calibrated magnifications. Images were stored onto MO-disks and contrast and brightness adjusted with Adobe Photoshop CS2 (Adobe Systems, Mountain View, CA, USA).

Acknowledgments

This work was supported in part by grants from the Deutsche Forschungsgemeinschaft (SPP1150 to T.E.B.S. and K.R. and SFB 621 to K.R.). Work by B.M. and W.D.H. was funded by UBS AG on behalf of a customer and by the Bonizzi-Theler Foundation. We thank Ken Campellone, Matt Welch and Giorgio Scita for reagents, Brigitte Denker for excellent technical assistance and Jürgen Wehland for support and providing infrastructure.

References

Benesch, S., Lommel, S., Steffen, A., Stradal, T.E., Scaplehorn, N., Way, M., *et al.* (2002). Phosphatidylinositol 4,5-biphosphate (PIP2)-induced vesicle movement depends on N-WASP and involves Nck, WIP, and Grb2. *J Biol Chem* **277,** 37771-37776.

Benesch, S., Polo, S., Lai, F.P., Anderson, K.I., Stradal, T.E., Wehland, J. and Rottner, K. (2005). N-WASP deficiency impairs EGF internalization and actin assembly at clathrin-coated pits. *J Cell Sci* **118,** 3103-3115.

Cain, R.J., Hayward, R.D. and Koronakis, V. (2008). Deciphering interplay between Salmonella invasion effectors. *PLoS pathogens* **4,** e1000037.

Campellone, K.G., Webb, N.J., Znameroski, E.A. and Welch, M.D. (2008). WHAMM is an Arp2/3 complex activator that binds microtubules and functions in ER to Golgi transport. *Cell* **134,** 148-161.

Chang, J., Chen, J. and Zhou, D. (2005). Delineation and characterization of the actin nucleation and effector translocation activities of Salmonella SipC. *Mol Microbiol* **55,** 1379-1389.

Cossart, P. and Sansonetti, P.J. (2004). Bacterial invasion: the paradigms of enteroinvasive pathogens. *Science* **304,** 242-248.

Criss, A.K. and Casanova, J.E. (2003). Coordinate regulation of Salmonella enterica serovar Typhimurium invasion of epithelial cells by the Arp2/3 complex and Rho GTPases. *Infect Immun* **71,** 2885-2891.

Czuchra, A., Wu, X., Meyer, H., van Hengel, J., Schroeder, T., Geffers, R., *et al.* (2005). Cdc42 is not essential for filopodium formation, directed migration, cell polarization, and mitosis in fibroblastoid cells. *Mol Biol Cell* **16,** 4473-4484.

Datsenko, K.A. and Wanner, B.L. (2000). One-step inactivation of chromosomal genes in Escherichia coli K-12 using PCR products. *Proc Natl Acad Sci U S A* **97,** 6640-6645.

Di Nardo, A., Cicchetti, G., Falet, H., Hartwig, J.H., Stossel, T.P. and Kwiatkowski, D.J. (2005). Arp2/3 complex-deficient mouse fibroblasts are viable and have normal leading-edge actin structure and function. *Proc Natl Acad Sci U S A* **102,** 16263-16268.

Elsinghorst, E.A. (1994). Measurement of invasion by gentamicin resistance. *Methods Enzymol* **236,** 405-420.

Goley, E.D. and Welch, M.D. (2006). The ARP2/3 complex: an actin nucleator comes of age. *Nat Rev Mol Cell Biol* **7,** 713-726.

Hardt, W.D., Chen, L.M., Schuebel, K.E., Bustelo, X.R. and Galan, J.E. (1998). S. typhimurium encodes an activator of Rho GTPases that induces membrane ruffling and nuclear responses in host cells. *Cell* **93,** 815-826.

Hayward, R.D. and Koronakis, V. (1999). Direct nucleation and bundling of actin by the SipC protein of invasive Salmonella. *Embo J* **18,** 4926-4934.

Heasman, S.J. and Ridley, A.J. (2008). Mammalian Rho GTPases: new insights into their functions from in vivo studies. *Nat Rev Mol Cell Biol* **9,** 690-701.

Hoiseth, S.K. and Stocker, B.A. (1981). Aromatic-dependent Salmonella typhimurium are non-virulent and effective as live vaccines. *Nature* **291,** 238-239.

Innocenti, M., Zucconi, A., Disanza, A., Frittoli, E., Areces, L.B., Steffen, A., *et al.* (2004). Abi1 is essential for the formation and activation of a WAVE2 signalling complex. *Nat Cell Biol* **6,** 319-327.

Katoh, H. and Negishi, M. (2003). RhoG activates Rac1 by direct interaction with the Dock180-binding protein Elmo. *Nature* **424,** 461-464.

Linardopoulou, E.V., Parghi, S.S., Friedman, C., Osborn, G.E., Parkhurst, S.M. and Trask, B.J. (2007). Human subtelomeric WASH genes encode a new subclass of the WASP family. *PLoS Genet* **3,** e237.

Lommel, S., Benesch, S., Rohde, M., Wehland, J. and Rottner, K. (2004). Enterohaemorrhagic and enteropathogenic Escherichia coli use different mechanisms for actin pedestal formation that converge on N-WASP. *Cell Microbiol* **6,** 243-254.

Lommel, S., Benesch, S., Rottner, K., Franz, T., Wehland, J. and Kuhn, R. (2001). Actin pedestal formation by enteropathogenic Escherichia coli and intracellular motility of Shigella flexneri are abolished in N-WASP-defective cells. *EMBO Rep* **2,** 850-857.

Machesky, L.M. and Insall, R.H. (1998). Scar1 and the related Wiskott-Aldrich syndrome protein, WASP, regulate the actin cytoskeleton through the Arp2/3 complex. *Curr Biol* **8,** 1347-1356.

May, R.C., Hall, M.E., Higgs, H.N., Pollard, T.D., Chakraborty, T., Wehland, J., *et al.* (1999). The Arp2/3 complex is essential for the actin-based motility of Listeria monocytogenes. *Curr Biol* **9,** 759-762.

McGhie, E.J., Hayward, R.D. and Koronakis, V. (2001). Cooperation between actin-binding proteins of invasive Salmonella: SipA potentiates SipC nucleation and bundling of actin. *Embo J* **20,** 2131-2139.

McGhie, E.J., Hayward, R.D. and Koronakis, V. (2004). Control of actin turnover by a salmonella invasion protein. *Mol Cell* **13,** 497-510.

Munter, S., Way, M. and Frischknecht, F. (2006). Signaling during pathogen infection. *Sci STKE* **335,** re5.

Norris, F.A., Wilson, M.P., Wallis, T.S., Galyov, E.E. and Majerus, P.W. (1998). SopB, a protein required for virulence of Salmonella dublin, is an inositol phosphate phosphatase. *Proc Natl Acad Sci U S A* **95,** 14057-14059.

Olazabal, I.M., Caron, E., May, R.C., Schilling, K., Knecht, D.A. and Machesky, L.M. (2002). Rho-kinase and myosin-II control phagocytic cup formation during CR, but not FcgammaR, phagocytosis. *Curr Biol* **12,** 1413-1418.

Patel, J.C. and Galan, J.E. (2005). Manipulation of the host actin cytoskeleton by Salmonella--all in the name of entry. *Curr Opin Microbiol* **8,** 10-15.

Patel, J.C. and Galan, J.E. (2006). Differential activation and function of Rho GTPases during Salmonella-host cell interactions. *J Cell Biol* **175,** 453-463.

Patel, J.C., Hueffer, K., Lam, T.T. and Galan, J.E. (2009). Diversification of a Salmonella virulence protein function by ubiquitin-dependent differential localization. *Cell* **137,** 283-294.

Perrett, C.A. and Jepson, M.A. (2009). Regulation of Salmonella-induced membrane ruffling by SipA differs in strains lacking other effectors. *Cell Microbiol* **11,** 475-487.

Pistor, S., Grobe, L., Sechi, A.S., Domann, E., Gerstel, B., Machesky, L.M., *et al.* (2000). Mutations of arginine residues within the 146-KKRRK-150 motif of the ActA protein of Listeria monocytogenes abolish intracellular motility by interfering with the recruitment of the Arp2/3 complex. *J Cell Sci* **113 (Pt 18),** 3277-3287.

Rottner, K., Stradal, T.E. and Wehland, J. (2005). Bacteria-host-cell interactions at the plasma membrane: stories on actin cytoskeleton subversion. *Dev Cell* **9,** 3-17.

Schlumberger, M.C. and Hardt, W.D. (2006). Salmonella type III secretion effectors: pulling the host cell's strings. *Curr Opin Microbiol* **9,** 46-54.

Shi, J., Scita, G. and Casanova, J.E. (2005). WAVE2 signaling mediates invasion of polarized epithelial cells by Salmonella typhimurium. *J Biol Chem* **280,** 29849-29855.

Snapper, S.B., Takeshima, F., Anton, I., Liu, C.H., Thomas, S.M., Nguyen, D., *et al.* (2001). N-WASP deficiency reveals distinct pathways for cell surface projections and microbial actin-based motility. *Nat Cell Biol* **3,** 897-904.

Steffen, A., Faix, J., Resch, G.P., Linkner, J., Wehland, J., Small, J.V., *et al.* (2006). Filopodia formation in the absence of functional WAVE- and Arp2/3-complexes. *Mol Biol Cell* **17,** 2581-2591.

Steffen, A., Rottner, K., Ehinger, J., Innocenti, M., Scita, G., Wehland, J. and Stradal, T.E. (2004). Sra-1 and Nap1 link Rac to actin assembly driving lamellipodia formation. *Embo J* **23,** 749-759.

Stender, S., Friebel, A., Linder, S., Rohde, M., Mirold, S. and Hardt, W.D. (2000). Identification of SopE2 from Salmonella typhimurium, a conserved guanine nucleotide exchange factor for Cdc42 of the host cell. *Mol Microbiol* **36,** 1206-1221.

Stevens, J.M., Galyov, E.E. and Stevens, M.P. (2006). Actin-dependent movement of bacterial pathogens. *Nat Rev Microbiol* **4,** 91-101.

Stradal, T.E. and Scita, G. (2006). Protein complexes regulating Arp2/3-mediated actin assembly. *Curr Opin Cell Biol* **18,** 4-10.

Takenawa, T. and Suetsugu, S. (2007). The WASP-WAVE protein network: connecting the membrane to the cytoskeleton. *Nat Rev Mol Cell Biol* **8,** 37-48.

Unsworth, K.E., Way, M., McNiven, M., Machesky, L. and Holden, D.W. (2004). Analysis of the mechanisms of Salmonella-induced actin assembly during invasion of host cells and intracellular replication. *Cell Microbiol* **6,** 1041-1055.

Wang, L. and Zheng, Y. (2007). Cell type-specific functions of Rho GTPases revealed by gene targeting in mice. *Trends Cell Biol* **17,** 58-64.

Wennerberg, K., Ellerbroek, S.M., Liu, R.Y., Karnoub, A.E., Burridge, K. and Der, C.J. (2002). RhoG signals in parallel with Rac1 and Cdc42. *J Biol Chem* **277,** 47810-47817.

Wheeler, A.P., Smith, S.D. and Ridley, A.J. (2006). CSF-1 and PI 3-kinase regulate podosome distribution and assembly in macrophages. *Cell Motil Cytoskeleton* **63,** 132-140.

Zhou, D., Chen, L.M., Hernandez, L., Shears, S.B. and Galan, J.E. (2001). A Salmonella inositol polyphosphatase acts in conjunction with other bacterial effectors to promote host cell actin cytoskeleton rearrangements and bacterial internalization. *Mol Microbiol* **39,** 248-259.

Zuchero, J.B., Coutts, A.S., Quinlan, M.E., Thangue, N.B. and Mullins, R.D. (2009). p53-cofactor JMY is a multifunctional actin nucleation factor. *Nat Cell Biol* **11,** 451-459.

Figure legends

Figure 1. WAVE-complex is not essential for *Salmonella* invasion. (**A**) VA-13 fibroblast cells stably suppressed for Nap1 expression (Nap1 RNAi) or control cells (Mock RNAi) were subjected to wildtype *Salmonella enterica* Serovar Typhimurium (*S. typhimurium* WT) or the isogenic, invasion–deficient mutant lacking SipB (*S. typhimurium* ΔSipB) as non-specific control. Data are arithmetic means ± standard errors of means (error bars) from at least four independent experiments each normalized to the uptake of wildtype bacteria by mock RNAi-treated controls. WAVE-complex knockdown does not abrogate bacterial entry specific to wildtype *Salmonella*. Two-sample t-tests confirmed no statistical difference for entry of wildtype *Salmonella* into control or Nap1 knockdown cells ($p \leq 0.6$). (**B**) Western Blotting demonstrating virtual absence of the WAVE-complex component Nap1 in Nap1 RNAi cells; tubulin was used as loading control.

Figure 2. WAVE-complex knockdown interferes with *Salmonella*-induced ruffling but not actin assembly. Confocal microscopy of VA-13 fibroblast cells stably suppressed for Nap1 expression (Nap1 RNAi) or control cells (Mock RNAi), infected with wildtype *Salmonella* (green) and stained for actin filaments (red). Three-dimensional (3D) reconstructions were computed from confocal sections (for animated 3D reconstructions of these cells see Supplementary Videos 1 and 2). Interactions and entry of the bacteria with mock RNAi cells are accompanied by generation of prominent lamellipodia and ruffles (arrows), which are absent upon Nap1 knockdown (arrowheads). Nevertheless, bacteria are still able to induce actin accumulations at bacterial contact and/or entry sites in Nap1 RNAi cells, which may aid the entry process. Bars equal 5µm.

Figure 3. Arp2/3-complex accumulation is not abolished in WAVE-complex-depleted cells. Mock-treated and stable Nap1 knockdown VA-13 fibroblasts were infected with wildtype *Salmonella typhimurium*, and labelled for the actin cytoskeleton (phalloidin, green in merge), the Arp2/3-complex component ArpC5 (p16) (red in merge), and *Salmonella* (blue in merge). Arp2/3-complex was recruited to sites of *Salmonella* invasion both in the presence (Mock RNAi) and absence (Nap1 RNAi) of WAVE-complex. Bars equal 10µm.

Figure 4. WAVE-complex depletion abrogates *Salmonella*-induced membrane ruffling. Mock and Nap1 RNAi VA-13 fibroblast cells were infected with wildtype *Salmonella typhimurium*, fixed and prepared for inspection by scanning electron microscopy. Note the dramatic induction of ruffles emanating from the dorsal surface of mock RNAi-treated fibroblasts challenged with *Salmonella* (rod-shaped objects). Ruffling is not induced in Nap1 RNAi cells. Instead, bacteria appear to be enveloped by the host cell surface in a "zipper-like" fashion. Bars equal 2µm.

Figure 5. N-WASP suppresses rather than promotes invasion of wildtype *Salmonella*. (**A**) N-WASP-expressing control (N-WASP$^{flox/flox}$) and corresponding knockout (N-WASP$^{del/del}$) fibroblast cell lines were subjected to gentamicin protection assay with wildtype (*S. typhimurium* WT) or invasion-deficient (*S. typhimurium* ΔSipB) bacteria. Data are arithmetic means ± standard errors of means (error bars) from at least four independent experiments each normalized to the uptake of wildtype bacteria by N-WASP$^{flox/flox}$ cells. Note specific *Salmonella* invasion to be increased upon genetic deletion of N-WASP (*****; two-sample t-test, statistically significant at $p \leq 0.022$). (**B**) Western Blotting demonstrating the absence of N-WASP in N-WASP$^{del/del}$ cells, and equal loading of cellular extracts as shown with tubulin antibody.

Figure 6. Simultaneous depletion of N-WASP and WAVE-complex does not significantly reduce *Salmonella* invasion. (**A**) *Salmonella* entry as assessed by gentamicin survival assay using wildtype or SipB-deficient bacteria in N-WASP knockout cells mock-treated (Mock RNAi) or transiently suppressed for Nap1 expression (Nap1 RNAi). Data are arithmetic means ± standard errors of means (error bars) from at least four independent experiments each normalized to the uptake of wildtype bacteria by mock RNAi-treated N-WASP$^{del/del}$ cells. Note only a modest reduction of specific *Salmonella* entry upon Nap1 knockdown in these cells, which was not statistically significant (two-sample t-test, $p \leq 0.14$). (**B**) Western Blotting demonstrating suppression of expression of WAVE-complex components in Nap1 knockdown cells (Nap1 and WAVE2), but not of Arp2/3-complex (exemplified by Arp3). Tubulin was used as loading control.

Figure 7. Arp2/3-complex targets to sites of *Salmonella* entry in the absence of both N-WASP and WAVE-complex. Control (Mock RNAi) and Nap1 knockdown (Nap1 RNAi) fibroblasts lacking N-WASP (N-WASP$^{del/del}$) were infected with wildype *Salmonella typhimurium*, and labelled for the actin cytoskeleton (phalloidin, green in merge), the Arp2/3-complex component ArpC5 (p16) (red in merge), and *Salmonella* (blue in merge). N-WASP-deficient cells are still capable of Arp2/3-complex accumulation at sites of *Salmonella* invasion, irrespective of the level of WAVE-complex expression. Bars equal 10µm.

Figure 8. Arp2/3-complex knockdown reduces *Salmonella* invasion. (**A**) N-WASP expressing control (N-WASP$^{flox/flox}$) and N-WASP knockout (N-WASP$^{del/del}$) fibroblasts were transiently transfected with mock, Arp3 or ArpC3 (p21) knockdown vectors as indicated, and tested for invasion efficiency of wildtype *Salmonella* or entry-deficient bacteria (ΔSipB) as control using gentamicin survival assay. Data are arithmetic means ± standard errors of means (error bars) from at least four independent experiments each normalized to the uptake of

wildtype bacteria by the respective mock RNAi-treated cells. Data were statistically compared using two-sample t-test (*; statistically significant at p≤0.004 and 0.005 for Arp3 and p21 RNAi in N-WASP$^{flox/flox}$ and p≤0.043 and 0.049 for Arp3 and p21 RNAi in N-WASP$^{del/del}$ cells). (**B**) Western Blotting documenting knockdown efficiency using specific antibodies as indicated and tubulin as loading control. Arp3 knockdown also suppresses p21 expression, but not *vice versa*.

Figure 9. WASH localizes to sites of *Salmonella* entry. NIH 3T3 cells expressing EGFP-tagged variants of WHAMM, JMY or WASH as indicated (green) were infected with *Salmonella*, counterstained for the actin cytoskeleton (phalloidin, red) and for bacteria (white) as indicated, and inspected by confocal microscopy (for comparison of EGFP control see Supplementary Figure 1). 3D reconstructions were computed from confocal sections. Note the absence of specific enrichment of WHAMM or JMY at actin accumulations and/or ruffles (arrowheads) accompanied by *Salmonella* invasion. In contrast, WASH can specifically co-localize with *Salmonella* at entry sites (arrows). Bars equal 5µm.

Figure 10. WASH is a novel Arp2/3-complex activator operating in *Salmonella* invasion. (**A**) Extracts from N-WASP knockout (N-WASP$^{del/del}$) and control (N-WASP$^{flox/flox}$) fibroblasts were assayed for WASH and tubulin expression using Western Blotting, and quantified. (**B**) Western Blots documenting suppression of WASH expression by RNA interference in both the presence (N-WASP$^{flox/flox}$) and absence (N-WASP$^{del/del}$) of N-WASP expression as indicated. (**C**) Mock and WASH siRNA-treated cells were subjected to gentamicin survival assay using wildtype *Salmonella* or entry-deficient control (ΔSipB) in the presence or absence of N-WASP as indicated. Data are arithmetic means ± standard errors of means (error bars) from at least four independent experiments each normalized to the uptake of wildtype bacteria by the respective mock RNAi-treated cells. Data were statistically compared using two-

sample t-test (*****; statistically significant at $p \leq 0.04$ and 0.03 for N-WASP$^{flox/flox}$ and N-WASP$^{del/del}$ cells, respectively.

Supplementary Figure 1. WAVE2 and N-WASP localize to sites of *Salmonella* entry. NIH 3T3 cells expressing EGFP alone as control or EGFP-WAVE2 or –N-WASP (green) were infected with *Salmonella*, counterstained for the actin cytoskeleton (phalloidin, red) and for bacteria (white) as indicated, and inspected by confocal microscopy. 3D reconstructions were computed from confocal sections. Note very weak enrichment of EGFP fluorescence in ruffles, apparently due to increase of cytosolic volume in these ruffles (arrowheads). Thus, accumulation of EGFP-tagged WAVE2 and N-WASP in *Salmonella*-induced ruffles at bacterial entry sites (arrows) was concluded to be largely specific. Bars equal 5µm.

Supplementary Figure 2. WAVE-complex knockdown interferes with *Salmonella*-induced ruffling but not actin assembly. VA-13 fibroblast cells stably suppressed for Nap1 expression (Nap1 RNAi) or control cells (Mock RNAi), infected with wildtype *Salmonella* (green) and stained for actin filaments (red) were recorded by widefield optics. *Salmonella* induce both local (arrowheads) and large global ruffles/lamellipodia (arrows) in mock RNAi cells, whereas solely local actin accumulations in Nap1 RNAi cells (double-headed arrowheads). Bars equal 10µm.

Supplementary Figure 3. Induction of ruffles and WAVE-complex-independent actin accumulations both require effector delivery. Confocal microscopy of VA-13 fibroblast cells stably suppressed for Nap1 expression (Nap1 RNAi) or control cells (Mock RNAi), infected with ΔSipB *Salmonella* (green) and stained for actin filaments (red). Three-dimensional (3D) reconstructions were computed from confocal sections. Note complete absence of any actin accumulations at bacteria-host interactions sites in both cell types. Bars equal 5µm.

Supplementary Figure 4. Residual WAVE-complex does not associate with actin accumulations induced in Nap1 knockdown cells. Stable mock-treated and Nap1 knockdown VA-13 fibroblasts were infected with wildype *Salmonella typhimurium*, and labelled for the actin cytoskeleton (phalloidin, green in merge), the WAVE-complex subunit Abi-1 (red in merge) and *Salmonella* (blue in merge). Abi-1 was clearly recruited to sites of *Salmonella* invasion in mock RNAi cells (arrows), but completely absent from those actin accumulations evoked by Salmonella in Nap1 RNAi cells (arrowheads). Bars equal 10µm.

Supplementary Figure 5. Arp2/3-complex accumulation requires effector delivery. Stable mock and Nap1 RNAi-treated VA-13 fibroblasts were infected with ΔSipB *Salmonella*, and labelled for the actin cytoskeleton (phalloidin, green in merge), the Arp2/3-complex component ArpC5 (p16) (red in merge), and *Salmonella* (blue in merge). No Arp2/3-complex recruitment was observed close to these bacteria lacking a functional type III secretion system. Bars equal 10µm.

Supplementary Figure 6. Arp2/3-complex recruitment in cells lacking N-WASP or both N-WASP and WAVE-complex is effector delivery-specific. Mock or Nap1 RNAi-treated N-WASP-deficient cells (N-WASP$^{del/del}$) were infected with ΔSipB *Salmonella*, and labelled for the actin cytoskeleton (phalloidin, green in merge), the Arp2/3-complex component ArpC5 (p16) (red in merge), and *Salmonella* (blue in merge).

Supplementary Figure 7. Transient WAVE-complex suppression does not significantly affect *Salmonella* entry. (**A**) Bacterial entry as assessed by gentamicin survival assay using wildtype or SipB-deficient bacteria in N-WASP$^{flox/flox}$ fibroblasts mock-treated (Mock RNAi) or transiently suppressed for Nap1 expression (Nap1 RNAi). Data are arithmetic means ±

standard errors of means (error bars) from at least four independent experiments normalized to the uptake of wildtype bacteria by mock RNAi-treated cells. Although statistically significant (*****; two-sample t-test, $p \leq 0.031$), the observed reduction upon transient Nap1 knockdown in these fibroblasts was quite modest. However, as these data contrasted the results after stable WAVE-complex suppression (Figure 1), they indicate at best a minor role of WAVE-complex in *Salmonella* entry in the context of fibroblast invasion. (**B**) Western Blotting demonstrating suppression of Nap1 and the WAVE-complex component WAVE2, but not N-WASP upon Nap1 knockdown; tubulin was used as loading control.

Supplementary Figure 8. Inhibition of actin polymerisation abolishes *Salmonella* invasion. (**A**) Fibroblasts (N-WASP$^{flox/flox}$) were treated with Latrunculin B (LatB) or vehicle as indicated, and infected with wildtpye *Salmonella* or the non-invasive mutant (*S. typhimurium* ΔSipB) as control. Data are arithmetic means ± standard errors of means (error bars) from at least four independent experiments normalized to the uptake of wildtype bacteria in vehicle-treated control cells. Note the complete abolishment of *Salmonella* invasion in LatB-treated cells (*****; two-sample t-test, statistically significant at $p \leq 0.0000$). (**B**) Equal amounts of cellular extracts for bacterial quantification were confirmed using tubulin antibody.

Supplementary Video 1. Animated 3D reconstruction of mock RNAi-treated VA-13 fibroblast infected with wildtype *Salmonella* (green) and counterstained with phalloidin (red).

Supplementary Video 2. Animated 3D reconstruction of Nap1 RNAi-treated VA-13 fibroblast infected with wildtype *Salmonella* (green) and counterstained with phalloidin (red)

Figure 1

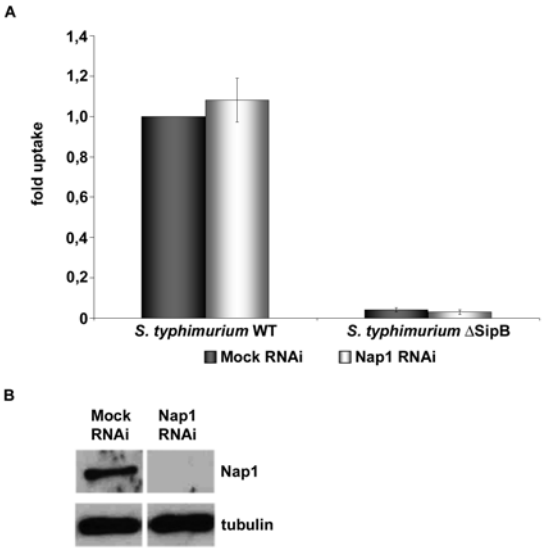
A
1,4
1,2
1,0
0,8
0,6
0,4
0,2
0
fold uptake
S. typhimurium WT
S. typhimurium ΔSipB
Mock RNAi
Nap1 RNAi
B
Mock RNAi
Nap1 RNAi
Nap1
tubulin

Figure 2

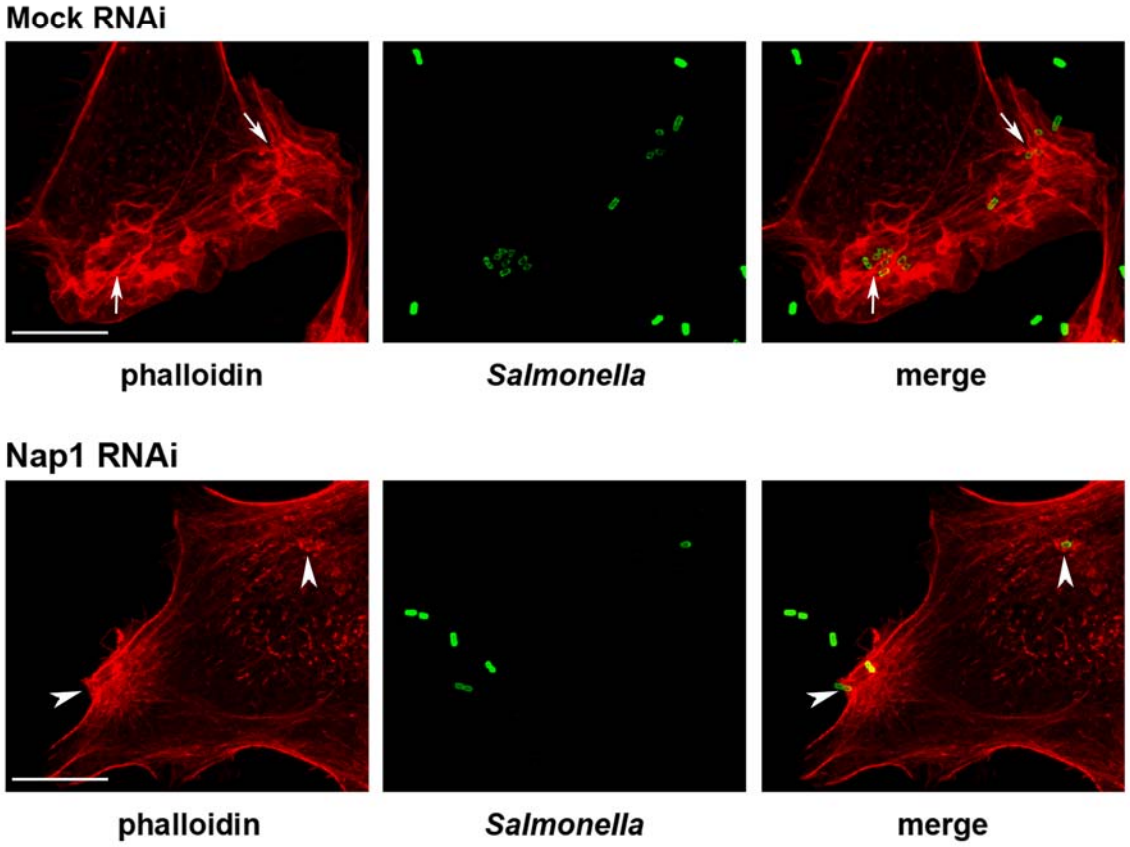
Mock RNAi
phalloidin
Salmonella
merge
Nap1 RNAi
phalloidin
Salmonella
merge

Figure 3

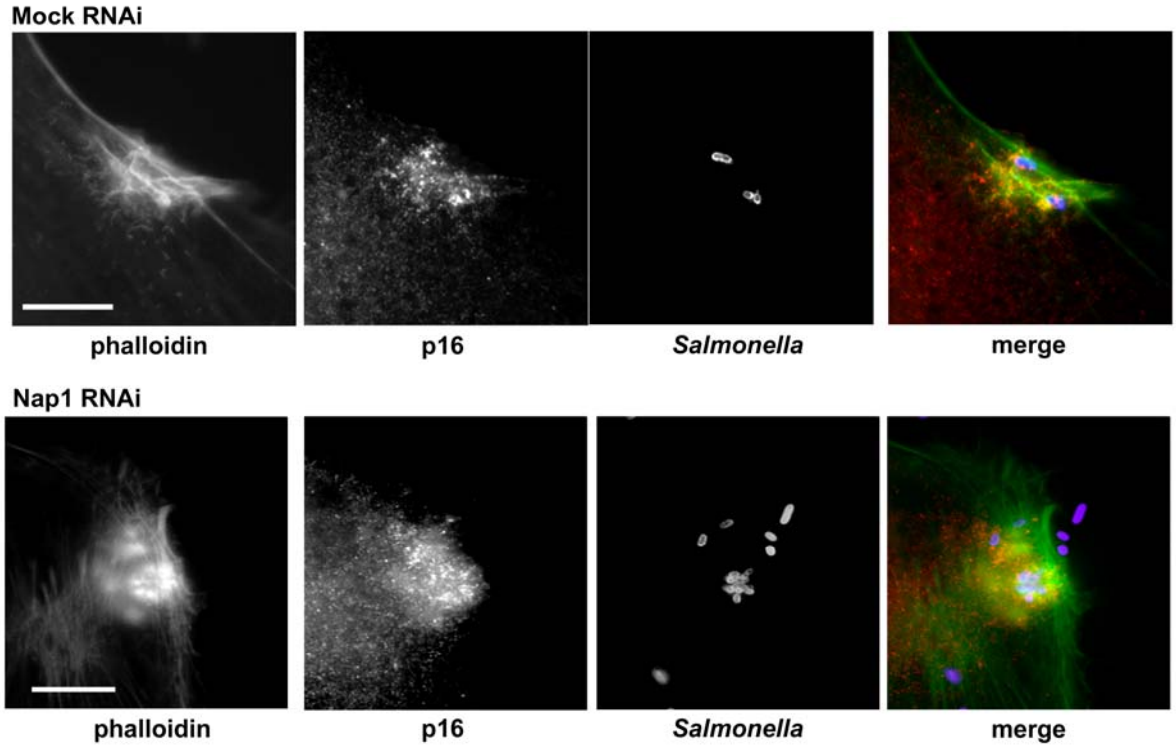
Mock RNAi
phalloidin
p16
Salmonella
merge
Nap1 RNAi
phalloidin
p16
Salmonella
merge

Figure 4

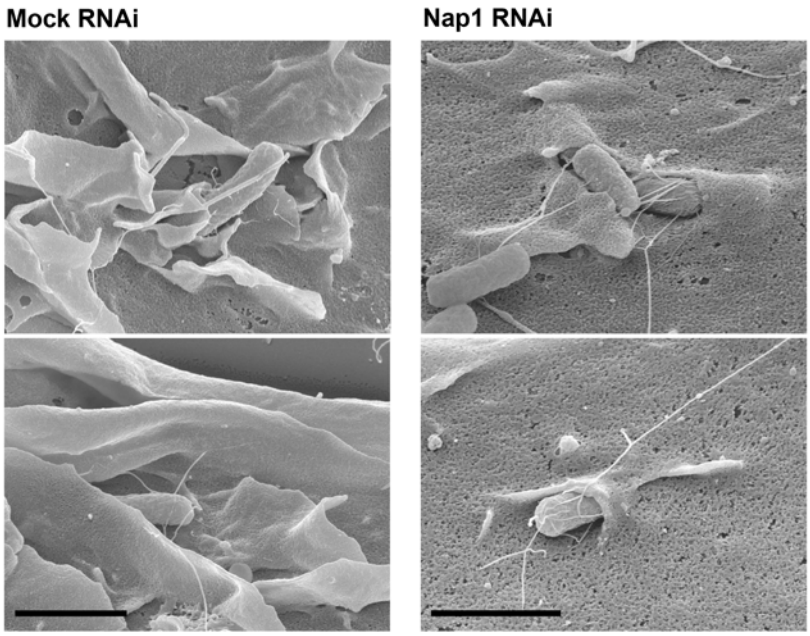

Figure 5

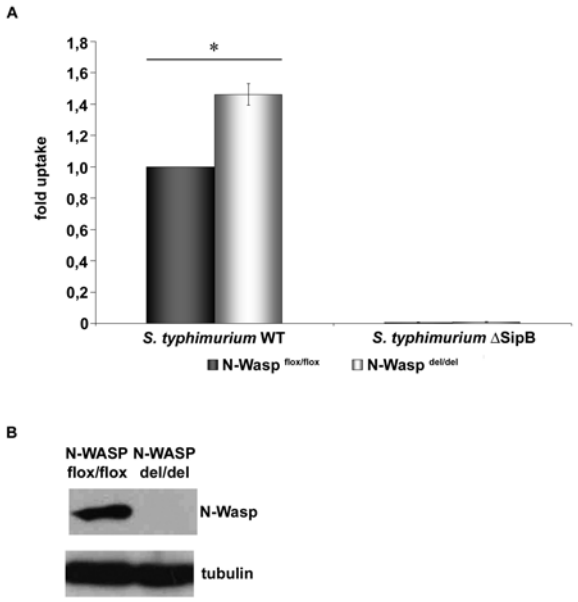
A
1,8
1,6
1,4
1,2
1,0
0,8
0,6
0,4
0,2
0
fold uptake
*
S. typhimurium WT
S. typhimurium ΔSipB
N-Wasp flox/flox
N-Wasp del/del
B
N-WASP flox/flox
N-WASP del/del
N-Wasp
tubulin

Figure 6

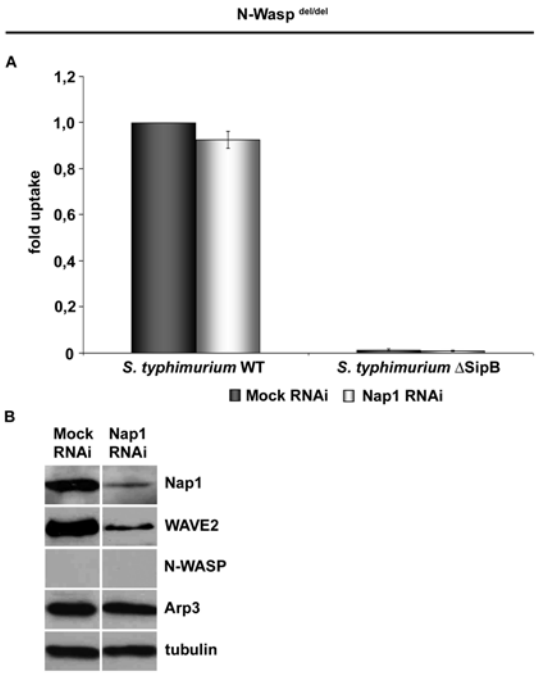
N-Wasp del/del
A
1,2
1,0
0,8
0,6
0,4
0,2
0
fold uptake
S. typhimurium WT
S. typhimurium ΔSipB
Mock RNAi
Nap1 RNAi
B
Mock RNAi
Nap1 RNAi
Nap1
WAVE2
N-WASP
Arp3
tubulin

Figure 7

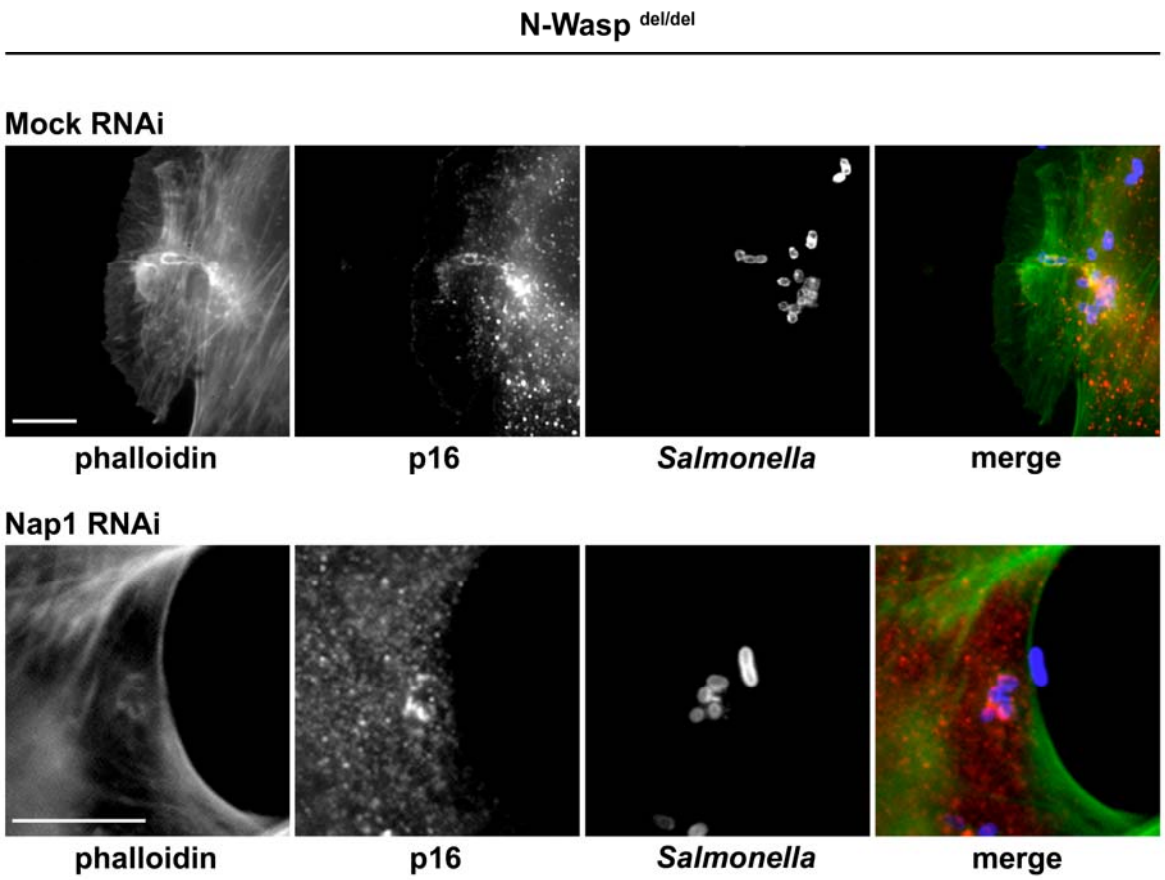
N-Wasp del/del
Mock RNAi
phalloidin
p16
Salmonella
merge
Nap1 RNAi
phalloidin
p16
Salmonella
merge

Figure 8

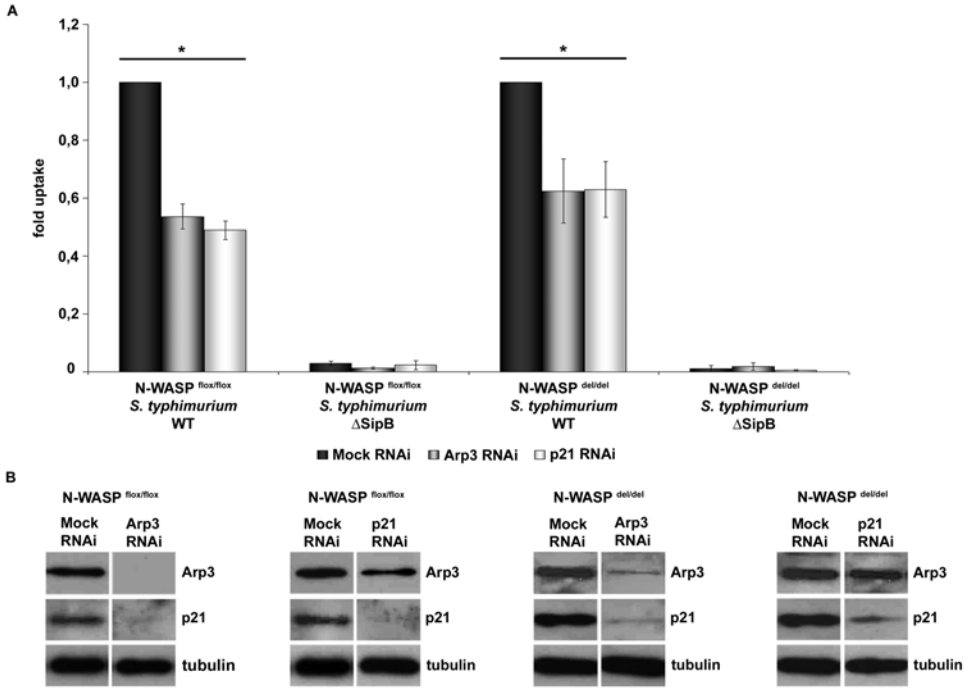
A
1,2
1,0
0,8
0,6
0,4
0,2
0
fold uptake
*
*
N-WASP flox/flox
S. typhimurium
WT
N-WASP flox/flox
S. typhimurium
ΔSipB
N-WASP del/del
S. typhimurium
WT
N-WASP del/del
S. typhimurium
ΔSipB
Mock RNAi
Arp3 RNAi
p21 RNAi
B
N-WASP flox/flox
Mock RNAi
Arp3 RNAi
Arp3
p21
tubulin
N-WASP flox/flox
Mock RNAi
p21 RNAi
Arp3
p21
tubulin
N-WASP del/del
Mock RNAi
Arp3 RNAi
Arp3
p21
tubulin
N-WASP del/del
Mock RNAi
p21 RNAi
Arp3
p21
tubulin

Figure 9

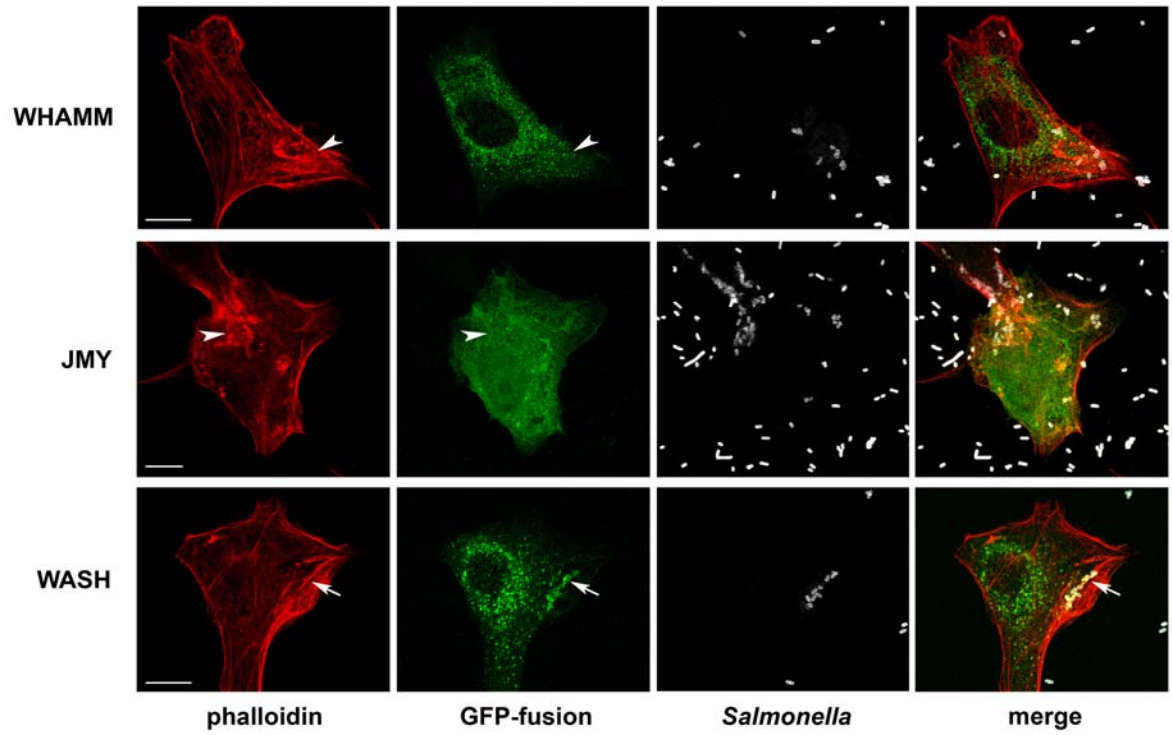

Figure 10

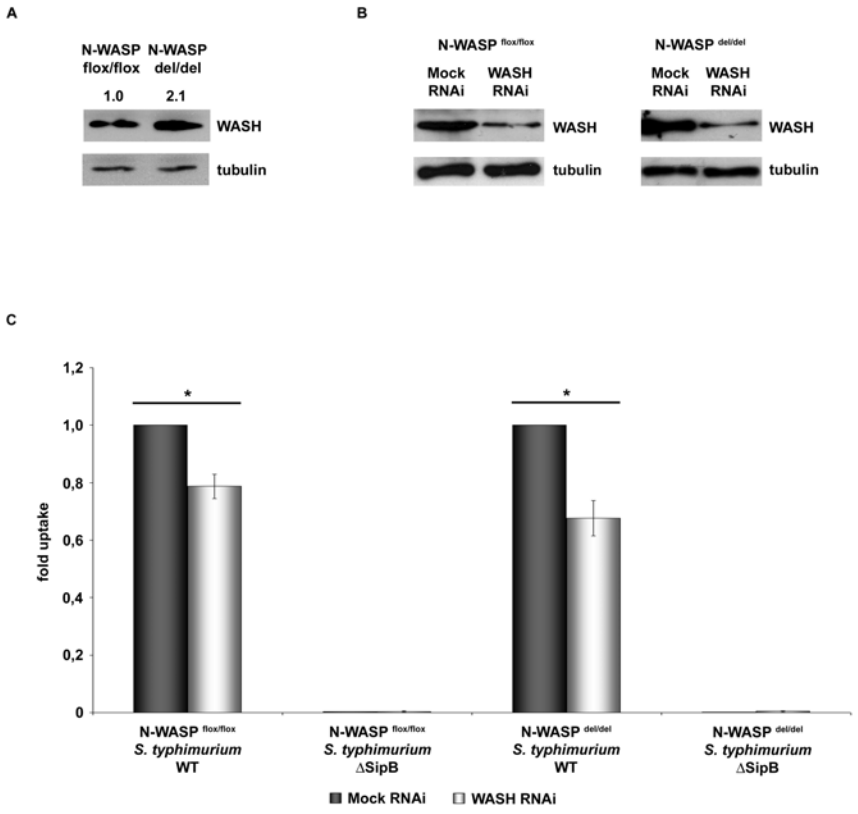
A
N-WASP flox/flox
N-WASP del/del
1.0
2.1
WASH
tubulin
B
N-WASP flox/flox
Mock RNAi
WASH RNAi
N-WASP del/del
Mock RNAi
WASH RNAi
WASH
tubulin
C
fold uptake
1,2
1,0
0,8
0,6
0,4
0,2
0
*
*
N-WASP flox/flox S. typhimurium WT
N-WASP flox/flox S. typhimurium ΔSipB
N-WASP del/del S. typhimurium WT
N-WASP del/del S. typhimurium ΔSipB
Mock RNAi
WASH RNAi

Supplementary Figure 1

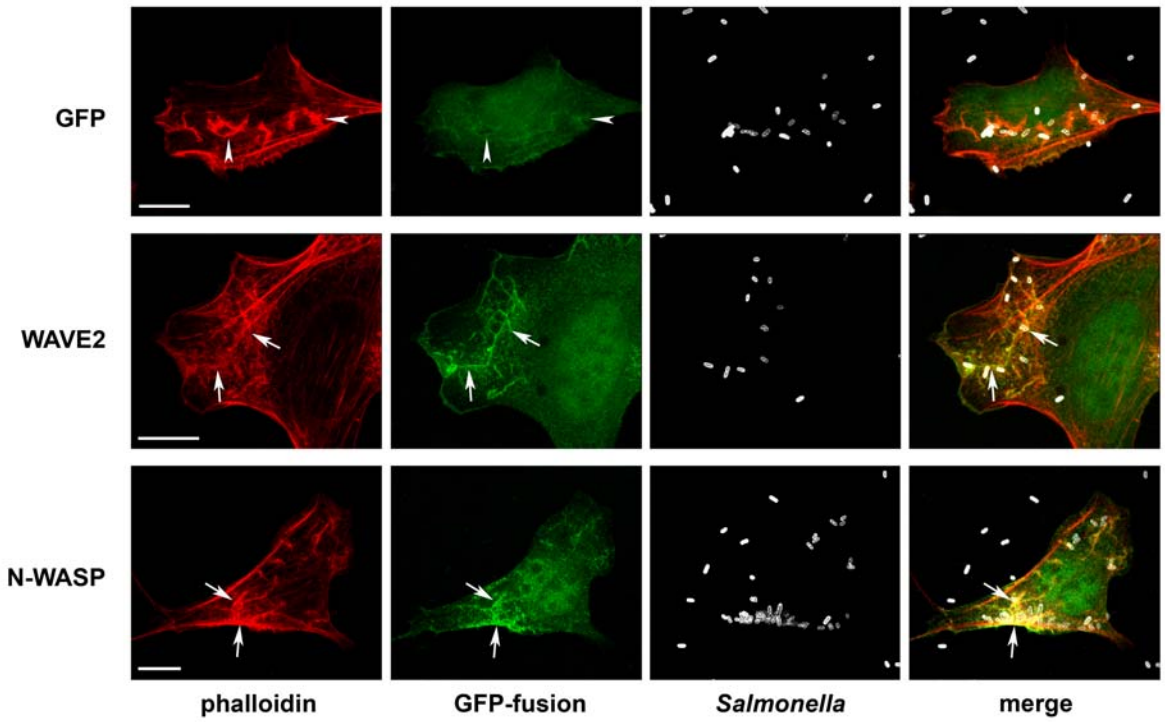

Supplementary Figure 2

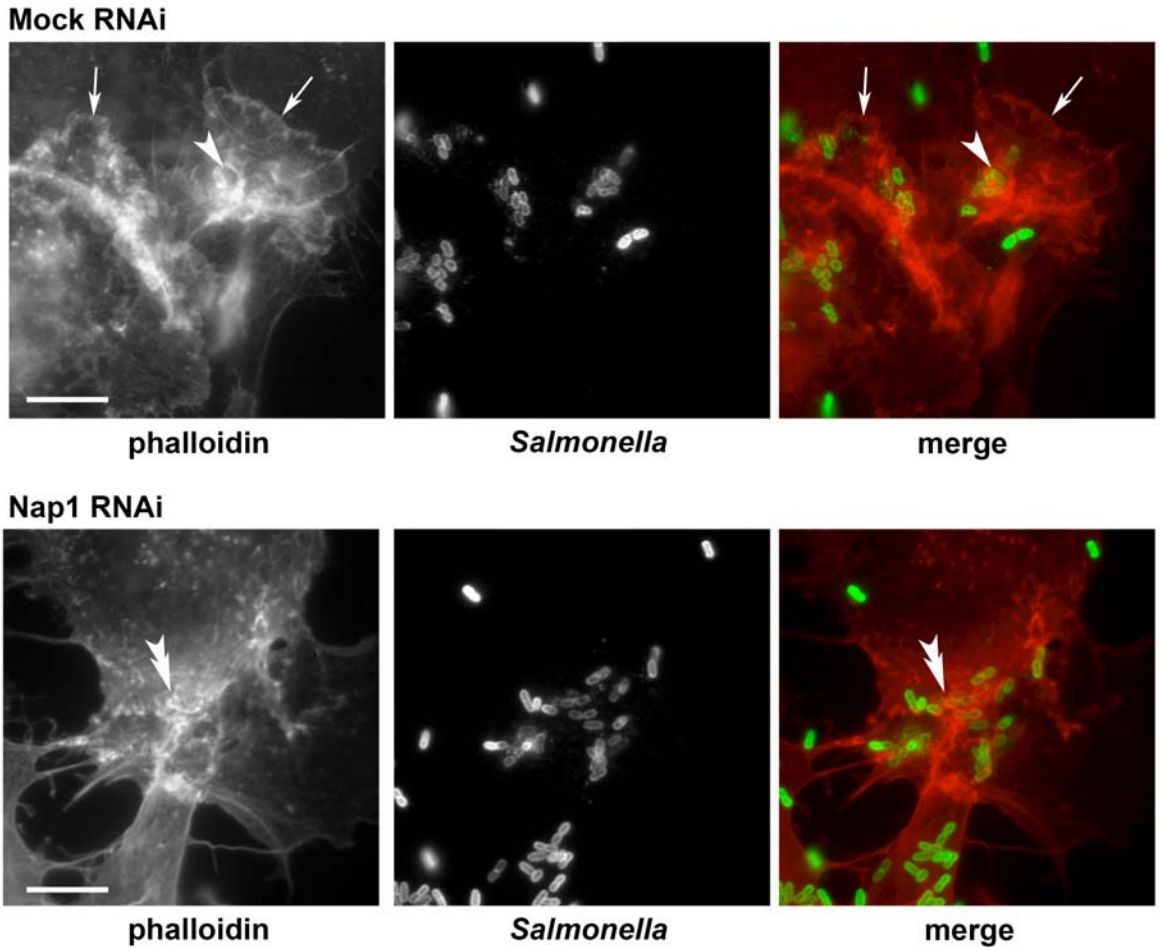

Supplementary Figure 3

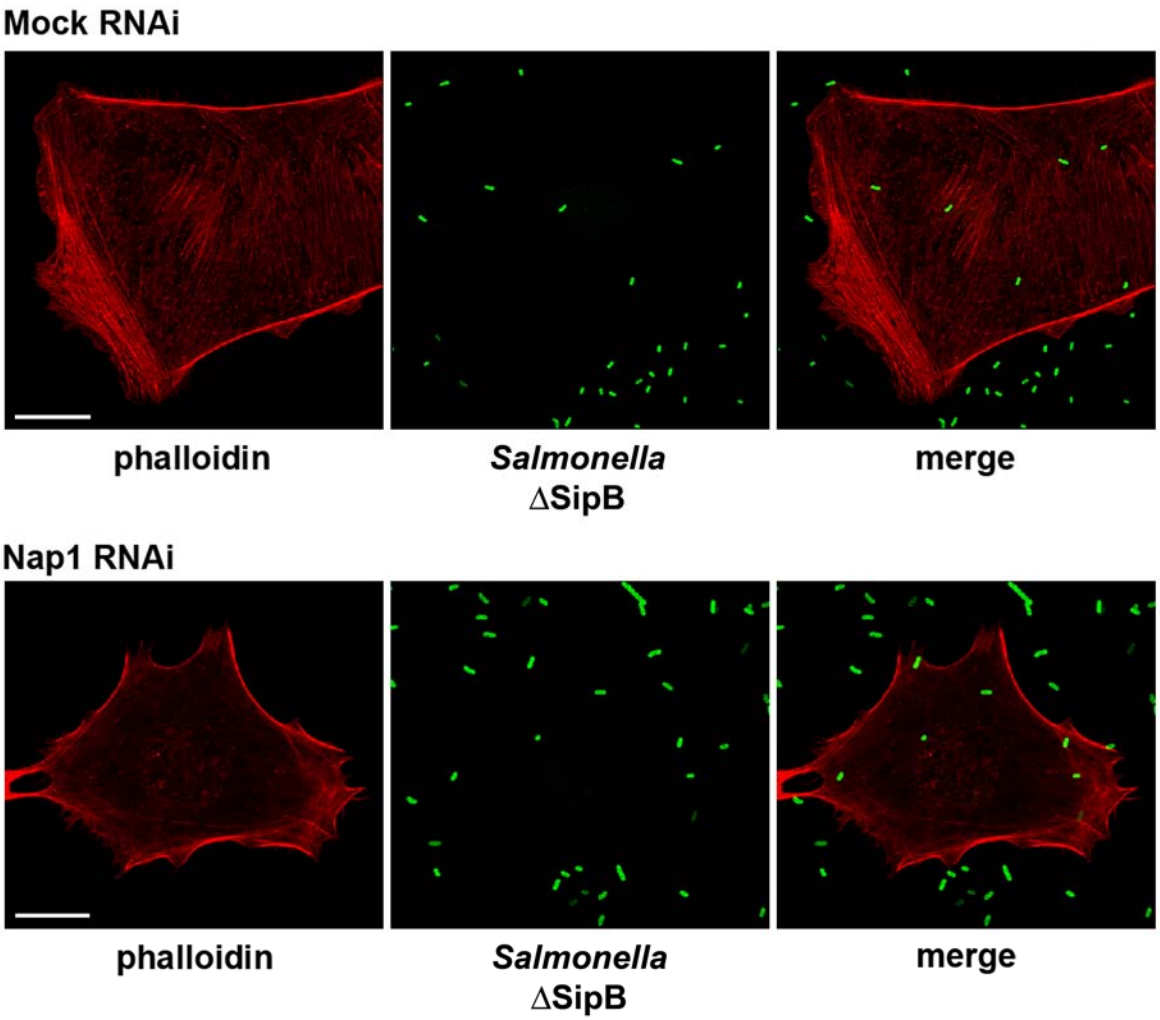

Supplementary Figure 4

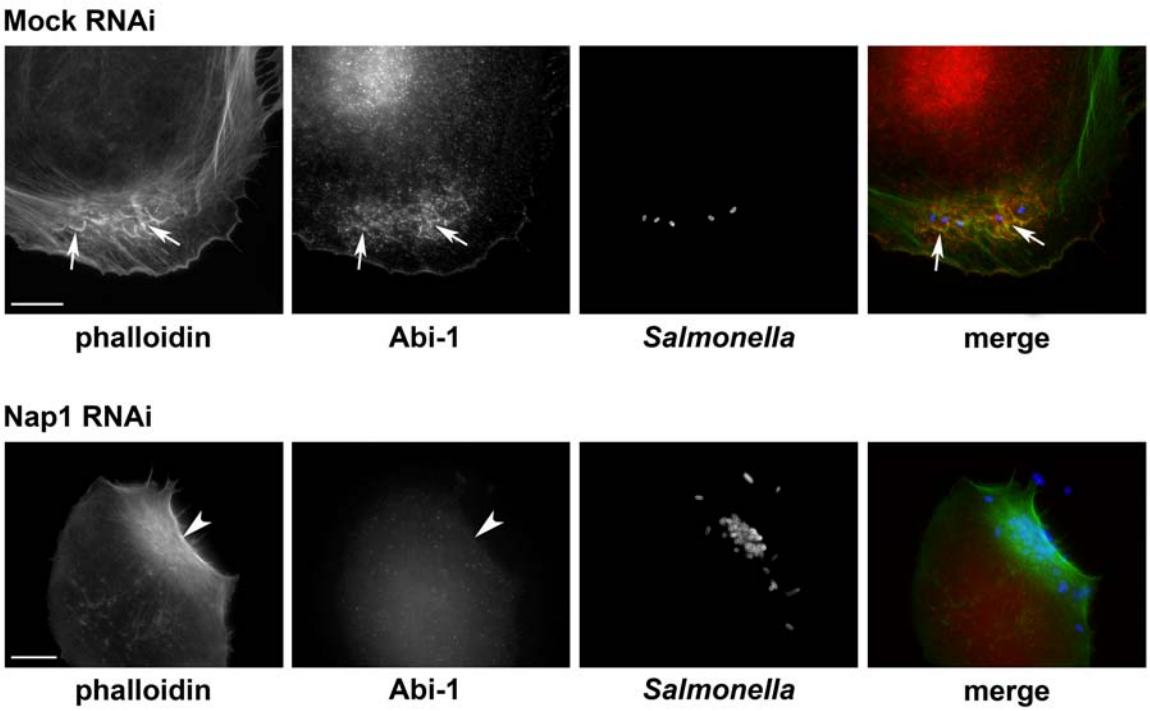

Supplementary Figure 5

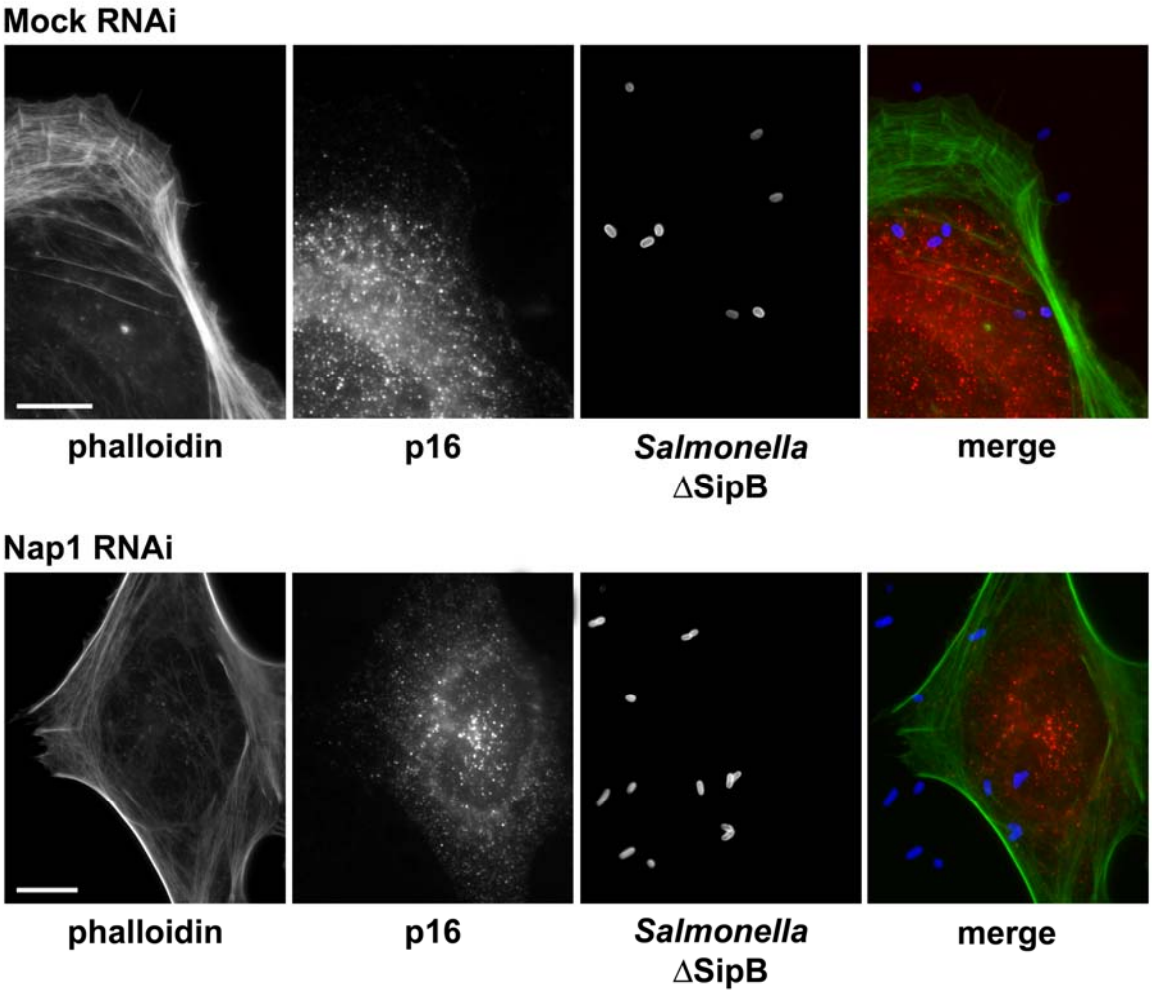

Supplementary Figure 6

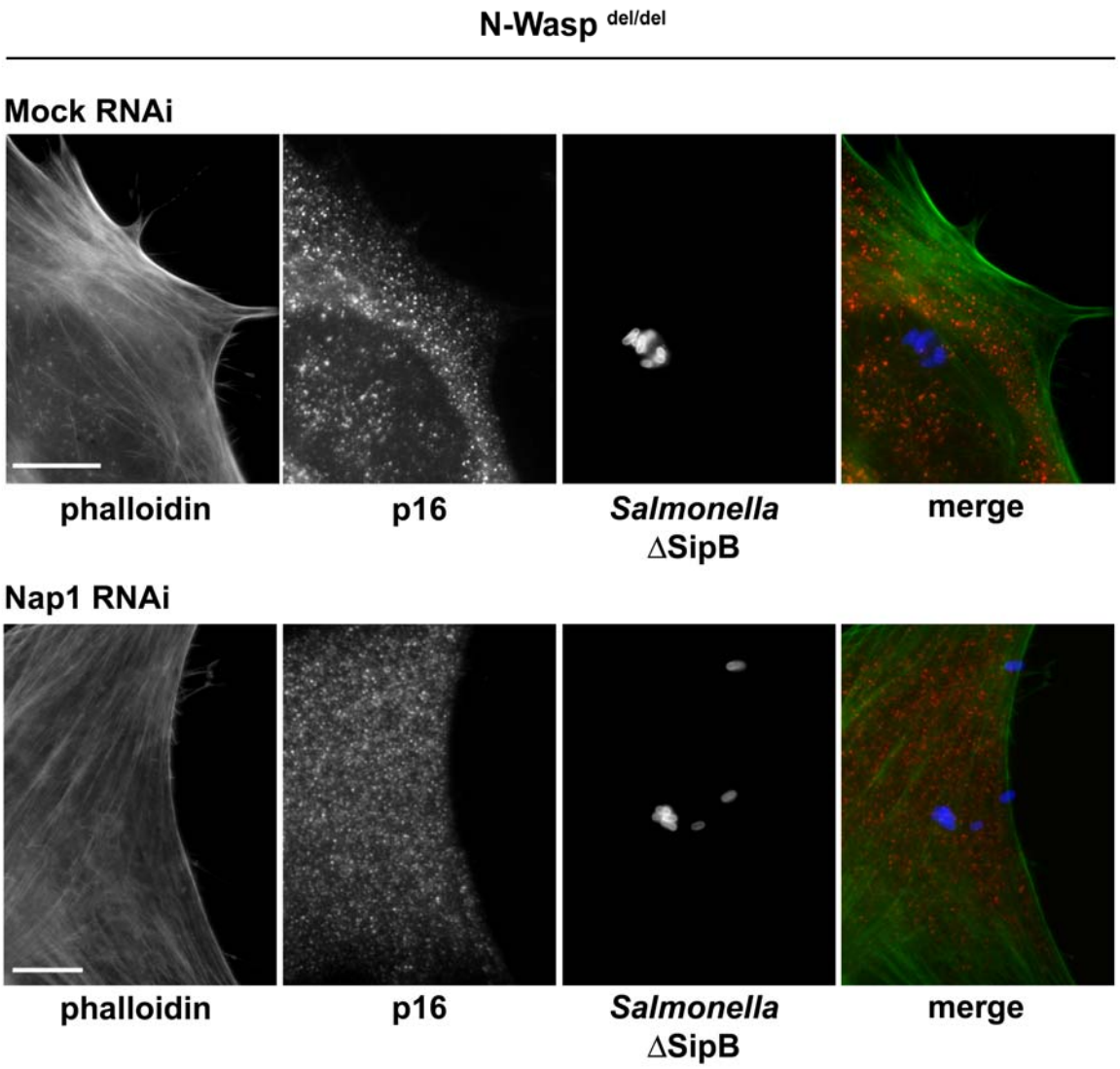

Supplementary Figure 7

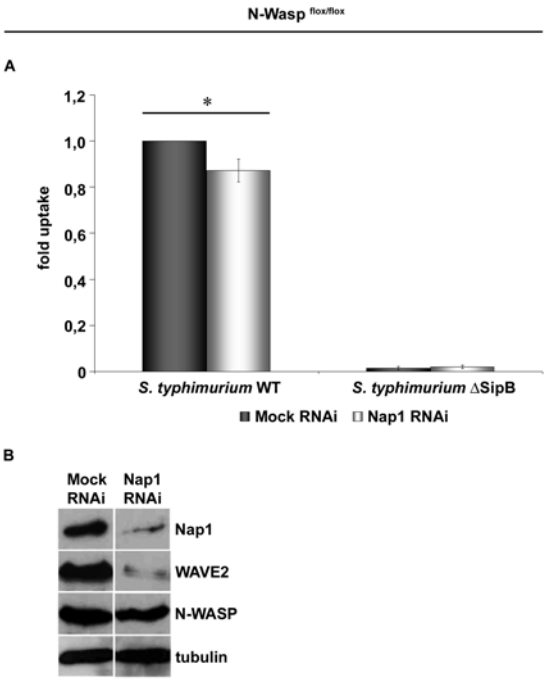

Supplementary Figure 8